Aberrant FGF19-FGFR4 Signal in Cancer

August 2020

Takashi FUTAMI

Aberrant FGF19-FGFR4 Signal in Cancer

A Dissertation Submitted to
the School of the Integrative and Global Majors,
the University of Tsukuba
in Partial Fulfillment of the Requirements
for the Degree of Doctor of Philosophy in Drug Discovery
(Doctoral Program in Life Science Innovation)

Takashi FUTAMI

Abstract

Cancer is one of the leading causes of death globally; about 1 in 6 deaths is due to cancer. The economic impact of cancer is significant and increasing.

Molecular-targeted therapies for cancer-based on the identification of oncogenic gene alterations and their specific inhibitors is associated with dramatic antitumor effect, reduced side effects, and improved patient survival. The molecular-targeted therapies include Herceptin for *epidermal growth factor receptor 2* amplification and overexpression in breast cancer patients, XALKORI for *echinoderm microtubule-associated protein-like 4–anaplastic lymphoma kinase* fusion oncogene-positive non–small-cell lung cancer, and Tarceva for *EGFR*-mutated non–small cell lung cancer.

The signaling pathway activated by FGFRs and their cognate ligands, i.e., fibroblast growth factors (FGF), plays an important role in the course of development from early embryogenesis to the formation of various organs. Aberrant activation of FGF/FGFR signaling promotes cellular proliferation, migration/invasion, and angiogenesis in a variety of human cancers. Different from FGFR1, 2 and 3, a limited number of oncogenic genetic alteration has been identified in FGFR4 and its physiological ligand, FGF19.

In this dissertation, aberrant FGF19-FGFR4 signals and therapeutic efficacy of FGFR inhibitor in cancer is investigated. In chapter II, the pharmacological profile of novel FGFR inhibitor, ASP5878, was investigated and explored its potential therapeutic efficacy on FGF19-expressing Hepatocellular carcinoma (HCC), aggressive cancer with poor prognosis. ASP5878 is a novel inhibitor of fibroblast growth factor receptors 1, 2, 3, and 4. It inhibits FGFR4 kinase activity with an IC50 of 3.5 nmol/L. ASP5878 potently suppressed the growth of the FGF19–expressing HCC cell lines Hep3B2.1-7, HuH-7, and JHH-7. In the Hep3B2.1-7 cell line, ASP5878 inhibited the phosphorylation of FGFR4 and its downstream signaling molecules as well as induced apoptosis. Oral administration of ASP5878 at 3 mg/kg induced sustained tumor regression in a subcutaneous xenograft mouse model using Hep3B2.1-7. In HuH-7, an orthotopic xenograft mouse model, ASP5878 induced complete tumor regression and dramatically extended the survival of the mice. These results suggest that ASP5878 is a potentially effective therapeutic agent for HCC patients with tumors expressing FGF19.

In Chapter III, a novel oncogenic *FGFR4* mutation in gastric cancer and investigated the function was investigated. Gastric cancer remains one of the leading causes of cancer death worldwide. Despite intensive investigations of treatments over the past three decades, the poor prognosis of patients with unresectable advanced or recurrent gastric cancer has not significantly changed, and improved therapies are required. The novel mutation, G636C-FGFR4 tyrosine kinase domain mutation was found in 1 of 83 primary human gastric tumors. The G636C mutation increased FGFR4 autophosphorylation, activated FGFR4 downstream signaling molecules, and enhanced anchorage-independent cell growth when expressed in NIH/3T3 cells. 3D-structural analysis and modeling of FGFR4 suggest that G636C destabilizes an auto-inhibitory conformation and stabilizes an active conformation, leading to increased kinase activation. Ba/F3 cell lines expressing the G636C-FGFR4 mutant were significantly more sensitive to ASP5878, a selective FGFR inhibitor, than the control. Oral administration of ASP5878 significantly inhibited the growth of tumors in mice engrafted with

G636C-FGFR4/3T3 cells. Together, our results demonstrate that mutationally activated FGFR4 acts as an oncoprotein. These findings support the therapeutic targeting of FGFR4 in gastric cancer.

In conclusion, these findings indicated that aberrant FGF19-FGFR4 signals in HCC and gastric cancer and that ASP5878 is a potentially effective therapeutic agent for cancer patients with tumors expressing FGF19 and G636C-FGFR4 mutations.

Contents

Abbreviations

ALK	Anaplastic lymphoma kinase
COSMIC	Catalogue Of Somatic Mutations In Cancer
EML4	Echinoderm microtubule-associated protein-like 4
ERK	Extracellular Signal-regulated Kinase
FDA	the Food and Drug Administration
FGF	Fibroblast growth factors
FGFR	Fibroblast growth factor receptor
FRS	FGFR substrate
GAPDH	glyceraldehyde-3-phosphate dehydrogenase
GRB2	growth factor receptor-bound 2
HCC	Hepatocellular carcinoma
HER2	epidermal growth factor receptor 2
HPSG	Heparran sulfate proteoglycans
Luc	luciferase
MAPK	mitogen activated protein kinase
MC	Methylcellulose
NSCLC	Non–small cell lung cancer
PARP	Poly（ADP-ribose）polymerase
PDB	protein database
PI3K	phosphoinositide-3-kinase
PLCγ	Phospholipase C gamma
RMS	rhabdomyosarcoma
STAT	signal transducer and activator of transcription
TCGA	The Cancer Genome Atlas
TK	Tyrosine kinase
VEGFR	Vascular Endothelial Growth Factor Receptor

Chapter I: General Introduction

Cancer is one of the leading causes of death globally and is responsible for an estimated 18.1 million new cases and 9.6 million deaths in 2018 (Bray et al., 2018). About 1 in 6 deaths is due to cancer worldwide, making the economic impact of cancer significant and increasing. The total cost of cancer care in 2020 is projected to be $173 billion (Mariotto et al., 2011). Cancer arises from the transformation of normal cells into tumor cells in a multistage process that generally progresses from a pre-cancerous lesion to a malignant tumor. These changes are the result of the interaction between a person's genetic factors and external agents.

There are many types of cancer treatment, including surgery, radiation, chemotherapy, immunotherapy, hormone therapy, stem cell transplant, and molecular-targeted therapy/precision medicine. Molecular-targeted therapies are based on the identification of oncogenic gene alterations and their specific inhibitors. Lee et al. have demonstrated dramatic antitumor effects with reduced side effects and improved patient survival compared to conventional therapies (Lee et al., 2018).

Many molecular-targeted cancer therapies have been approved by the Food and Drug Administration (FDA) to treat specific types of cancers including breast, leukemia, colorectal, lung, and ovarian cancers (Lee et al., 2018). The development of targeted therapies requires the identification of ideal targets, such as oncogene that cancer cells are addicted to their growth and survival.

One approach to identify potential targets is to compare the amounts of individual proteins in cancer cells with those in normal cells. Proteins that are present or more abundant in cancer cells but not in normal cells could be potential targets, especially if they are known to be involved in cell growth or survival. The *human epidermal growth factor receptor 2 protein (HER2) is* one of the examples of the differentially expressed targets. *HER2* is expressed at high levels in some cancer cells compared to normal cells. Several targeted therapies are directed against HER2, including trastuzumab, which is approved to treat certain breast and stomach cancers that overexpress *HER2* (Bang et al., 2010; Romond et al., 2005).

Another approach to find potential targets is to discover the genes that cause the production of mutant (genetically altered) proteins that drive cancer progression. For example, mutated EGFR, one of the cell growth signaling related proteins, is present in non–small cell lung cancer (NSCLC). These mutated EGFR forms are constitutively active and work as oncogenic driver. Tarceva targets this mutant form of the EGFR protein and is approved to treat patients with EGFR-mutated NSCLC (Pao et al., 2004).

Another approach is to identify abnormalities in chromosomes that are present in cancer cells but not in normal cells. Chromosome abnormalities result in the creation of a fusion gene as a gene that incorporates parts of two different genes, and its translated fusion protein may activate the protein constitutively and drive cancer development. Such fusion proteins are potential targets for targeted cancer therapies. For example, *echinoderm microtubule-associated protein-like 4–anaplastic lymphoma kinase (EML4-ALK)* fusion is one of the oncogenes in NSCLC. EML4-ALK is a fusion of the scaffold protein EML4 and the kinase protein ALK. The EML4-ALK fusion protein constitutively

activates ALK kinase by forming a coiled-coil domain in the EML4 region. XALKORI is an FDA approved drug for EML4-ALK fusion oncogene-positive NSCLC (Malik et al., 2014).

The FGF-FGFR signaling pathway plays a key role in the course of development from early embryogenesis to the formation of various organogenesis and tissue patterning, angiogenesis, and metabolism homeostasis (Belov and Mohammadi, 2013; Ornitz and Itoh, 2015). Eighteen genes encoding *FGFs* and four genes encoding *FGFR*, which are expressed in various cells. FGF superfamily is categorized into six subfamilies based on sequence homology and phylogeny. Those are FGF1 subfamily (*FGF1 and FGF2*), FGF4 subfamily (*FGF4, FGF5, and FGF6*), FGF7 subfamily (*FGF3, FGF7, FGF10, and FGF22*), FGF8 subfamily (*FGF8, FGF17, and FGF18*), FGF9 subfamily (*FGF9, FGF16, and FGF20*) and FGF19 subfamily (*FGF19, FGF21 and FGF23*) (Beenken and Mohammadi, 2009; Belov and Mohammadi, 2013). The first five subfamilies work as paracrine factors and regulate embryogenesis, organogenesis, and tissue patterning. On the other hands, the FGF19 subfamily regulates metabolic homeostasis and works as hormone-like endocrine manner to regulate bile acid, cholesterol, glucose, vitamin D and phosphate homeostasis (Fu et al., 2004; Kharitonenkov et al., 2005; Razzaque and Lanske, 2007; Tomlinson et al., 2002). Cell-surface heparan sulfate proteoglycans (HPSGs) stabilize the FGF ligand–receptor interaction to escape from protease-mediated degradation. In the case of FGF19 subfamily, the FGF–FGFR interaction requires a cell surface co-receptor, klotho or β-klotho, for high-affinity binding and signaling (Beenken and Mohammadi, 2009; Belov and Mohammadi, 2013).

FGFRs consist of three domains, an extracellular domain with three extracellular immunoglobulin-like domains (D1–D3), a transmembrane domain, and an intracellular tyrosine kinase domain. The D1 domain works as receptor autoinhibition. The D2 domain has a function of a docking site for the extracellular HPSGs. The D2 and D3 domains have an important role for ligand binding and specificity. Specificity for the different FGF ligands is provided by exclusive alternate splicing processes of the D3 domain (Johnson et al., 1991). Upon FGF binding to FGFR, the activation of the FGF-FGFR-HPSG/Klotho complex leads to an FGFR dimerization, structural conformational changes, then intermolecular transphosphorylation of kinase domain. The two main substrates of FGFR are FGFR substrate 2 (FRS2) and phospholipase C (PLC γ1). FRS2 binds the juxta-membrane domain of FGFR with son-of-sevenless (SOS) and growth factor receptor-bound 2 (GRB2), which activate multiple downstream transduction pathways such as mitogen-activated-protein-kinase (MAPK) and phosphoinositide-3-kinase (PI3K) -Akt signaling pathway. PLCγ1 phosphorylation leads to further activation of the MAPK pathway by RAF phosphorylation, p38 MAPK and Jun N-terminal kinase (JNK) pathways, signal transducer and activator of transcription (STAT) signaling, and ribosomal protein S6 kinase (Beenken and Mohammadi, 2009; Belov and Mohammadi, 2013)·(Turner and Grose, 2010).

Aberrantly activated FGFR signalings have been identified in several ways: amplification, fusion, or mutations of FGFR family members (Gallo et al., 2015; Helsten et al., 2016; Tanner and Grose, 2016). Oncogenic genetic alterations are identified in FGFR1, 2, 3, and 4 in human cancers. For example, *FGFR1* amplifications are identified in breast, lung, gastric, and bladder cancers (Campbell et al., 2016; Luo et al., 2017; Peifer et al., 2012; Weiss et al., 2010). *FGFR2* amplification,

mutations, and fusions are identified in breast, liver, uterine, lung, and gastric cancer (Tchaicha et al., 2014; Turner et al., 2010; Wu et al., 2013). *FGFR3* mutations and fusions are identified in bladder and lung cancers (2014; Gao et al., 2018; Wu et al., 2013). On the other hand, oncogenic genetic alteration of *FGFR4* is infrequently identified in cancers. FGFR4-N535K/D and V550E/L, were identified as oncogenic mutations in rhabdomyosarcoma (RMS), although other oncogenic alterations are unknown (Taylor et al., 2009). *FGF19* gene amplification has been identified in several cancers, including HCC, head and neck cancer and breast cancer (Lang et al., 2019). Previous studies have demonstrated that FGF19 amplification/overexpression could be oncogenic gene alteration in HCC (Miura et al., 2012, Hagel et al., 2015; Hierro et al., 2015).

As no FDA-approved drug that inhibits FGFR4 is available before this study, FGFR4 inhibitor is needed to be developed. Astellas has established assay systems including *in vitro* kinase activity assays, kinase selectivity assay, anti-tumor effect evaluation system (*in vitro, in vivo*), pharmacodynamics, pharmacokinetics, and safety assays. Screening of chemical libraries had been executed and more potent compounds have been developed through these assay systems based on structure-activity-relationships, crystal structure, and 3D modeling. Finally, ASP5878, novel and selective FGFR1/2/3/4 inhibitor, was identified as clinical candidate compounds.

Anti-tumor efficacy and preclinical profile of ASP5878 has been demonstrated in FGF19-expressing HCC in chapter II. To maximize the potency of ASP5878, other potential indications have been explored to identify novel an oncogenic gene alteration in FGF19-FGFR4 signal other than RMS. Several novel FGFR4 mutations has been identified in several cancers, including G636C in gastric cancer. The mechanism and oncogenicity of G636C-FGFR4 are demonstrated in Chapter III. There are huge unmet clinical needs in HCC and gastric cancer and effective therapeutic approaches with low side effects are urgently required, such as precision medicine. Identification of oncogenic gene alteration and its inhibitor would provide huge benefits for HCC and gastric cancer patients.

In summary, the objectives of this dissertation are to investigate the mechanism of aberrant FGF19-FGFR4 signal in cancer, especially for HCC and gastric cancer, and to demonstrate the therapeutic effect of novel FGFR inhibitor, ASP5878, in preclinical models.

Chapter II: ASP5878, a Novel Inhibitor of FGFR1, 2, 3, and 4, Inhibits the Growth of FGF19-Expressing Hepatocellular Carcinoma.

1. Introduction

HCC is aggressive cancer with poor prognosis and the third most common cause of cancer-related deaths worldwide (Murray et al., 2012). Chronic liver diseases, such as cirrhosis caused by infection of hepatitis B (HBV) and/or hepatitis C (HCV), alcohol consumption, and non-alcoholic steatohepatitis (NASH), is the important risk factor for the development of HCC. There are several treatments for HCC, including surgery, liver transplantation, radiation therapy, chemoembolization, radioembolization, heat ablation, immunotherapy, and molecular-target therapy. Surgical resection is the most successful treatment for early-stage HCC. However, 70% of patients have a recurrence after 5 years (Poon, 2011; Spangenberg et al., 2009). Sorafenib, a multi-kinase inhibitor, including Raf, VEGFRs, PDGFRs, cKIT, FLT3, and RET, has been approved as a d drug and standard therapy for surgically unresectable HCC and has been shown to improve the median survival from 7.9 months in patients receiving placebo to 10.7 months in a phase III trial by FDA (Cheng et al., 2009). However, side effects make sorafenib treatment difficult to continue, such as anorexia, nausea, vomiting, weight loss, and hypertension. More effective therapeutic approaches with low side effects are urgently required for unresectable HCC, such as precision medicine.

The FGF-FGFR signaling pathway plays an key role in the course of development from early embryogenesis to the formation of various organogenesis and tissue patterning, angiogenesis and metabolism homeostasis (Belov and Mohammadi, 2013; Ornitz and Itoh, 2015). FGF19 subfamily that is consist of *FGF19, FGF21 and FGF23*, regulate metabolism homeostasis and works as hormone like endocrine manner to regulate bile acid, cholesterol, glucose, vitamin D and phosphate homeostasis (Fu et al., 2004; Kharitonenkov et al., 2005; Razzaque and Lanske, 2007; Tomlinson et al., 2002). FGF19 is a physiologic ligand for FGFR4, which is expressed in and secreted from the small intestine and gallbladder, but not normal liver, and controls the cholesterol catabolism in the liver through FGFR4 and coreceptor, βKlotho (Beenken and Mohammadi, 2009). Furthermore, it has been reported that FGF19 is involved in several types of cancers such as HCC and colon cancer (Lin and Desnoyers, 2012; Sawey et al., 2011). Especially, *FGF19* gene amplification in liver is involved in 14% of HCC patients, and overexpression of *FGF19* in liver has been observed in about 50% of HCC patients (Desnoyers et al., 2008; Hyeon et al., 2013; Kharitonenkov et al., 2005). *FGF19* expression in liver correlates with poorer prognosis, recurrence, and tumor progression in HCC patients (Johnson et al., 1991; Miura et al., 2012). FGF19-expressing transgenic mice spontaneously develop HCC (Nicholes et al., 2002). The knockout of *FGFR4 gene* of the FGF19-expressing transgenic mice inhibited HCC development. This suggests that FGFR4 is essentially required for tumorigenesis in this FGF19-mediated HCC model (French et al., 2012). Furthermore, the cell proliferation of HCC cell lines with *FGF19* gene amplification is inhibited by the addition of FGF19-neutralizing antibodies, an RNAi that targets FGFR4, or FGFR4 inhibitors (Kharitonenkov et al., 2005; Miura et al., 2012), (Hagel et al., 2015; Hierro et al., 2015).

In chapter II, the preclinical profile of ASP5878, which is a novel FGFR-selective inhibitor,

targeting FGF19-expressing HCC is investigated. In addition, it has been demonstrated that ASP5878 suppressed the growth of FGF19-expressing HCC cell lines, accompanied by the inhibition of FGFR4 phosphorylation and its downstream signaling molecules, which led to the induction of apoptosis. Furthermore, it has been shown that the oral administration of ASP5878 induced sustained tumor regression in FGF19-expressing HCC mouse models. These data indicate that ASP5878 is a potentially effective therapeutic agent for HCC patients with tumors expressing FGF19.

2. Materials and methods

2.1 Compounds

ASP5878 (Astellas Pharma Inc. (Asaumi M, 2013)) and sorafenib were synthesized in-house. ASP5878 was dissolved in dimethyl sulfoxide for *in vitro* experiments or suspended in 0.5% methyl cellulose (MC) for *in vivo* experiments. Sorafenib was suspended in 12.5% Cremophor EL/12.5% ethanol for *in vivo* experiments.

2.2 Kinase assay

Inhibitory activities of 128 serine/threonine kinases were measured using the Mobility Shift Assay Kit (Carna Biosciences). IC_{50} values were determined for kinases that were inhibited by more than 50% by 200 nmol/L of ASP5878.

2.3 Cell growth assay

The human HCC cell lines HuH-7 (JCRB0403; ref.(Nakabayashi et al., 1982)), HUH-6 Clone 5 (JCRB0401; ref. (Doi, 1976)), HLF (JCRB0405; ref. (Dor et al., 1975)), huH-1 (JCRB0199; ref. (Huh and Utakoji, 1981)), JHH-1 (JCRB1062; ref. (Homma, 1985)), JHH-2 (JCRB1028; ref. (Homma, 1985)), JHH-5 (JCRB1029; ref. (Homma, 1985)), JHH-6 (JCRB1030; ref. (Homma, 1985)), and JHH-7 (JCRB1031; ref. (Homma, 1985)) were obtained from the Health Science Research Resources Bank. Hep3B2.1-7 (HB-8064), SNU-423 (CRL-2238; ref. (Park et al., 1995)), SNU-449 (CRL-2234; ref. (Park et al., 1995)), SNU-182 (CRL-2235; ref. (Park et al., 1995)), SNU-387 (CRL-2237; ref. (Park et al., 1995)), SNU-398 (CRL-2233; ref. (Park et al., 1995)), HepG2 (HB-8065), and MDA-MB-453 (HTB-131) were obtained from the American Type Culture Collection. Li-7 (RCB1941) was obtained from RIKEN Bioresource Center. SNU-739 and SNU-368 were obtained from the Korean Cell Line Bank. PLC/PRF/5 was obtained from DS Pharma Biomedical. HCC cell lines were cultured according to each manufacturer's guideline. The cell lines in this study were not authenticated by any tests in our laboratory but were purchased from the providers of authenticated cell lines and stored at early passages in a central cell bank at Astellas Pharma Inc. The experiments were conducted using low-passage cultures of these stocks. The cells were seeded in 96-well plates and incubated overnight. The cells were treated with ASP5878 for 5 days. Cell viability was measured using CellTiter-Glo (Promega).

2.4 Western blotting, ELISA, and pharmacodynamics

HCC cell lines were lysed with cell lysis buffer containing phosphatase and protease inhibitors, and the protein levels of FGF19, FGFR4, βKlotho, and actin (Clone AC-74) were determined by immunoblotting. Hep3B2.1-7 cells were treated with ASP5878 for 2 hours, and the protein levels of phospho-FRS2 (Tyr436), FRS2, phospho-extracellular signal-regulated kinase (phospo-ERK), ERK, glyceraldehyde-3-phosphate dehydrogenase (GAPDH), and actin (Clone AC-74) were detected by immunoblotting. Phosphorylated FGFR4 and total FGFR4 were measured by immunoprecipitation using FGFR4 antibody (A10) or mouse IgG_1 isotype control, followed by immunoblotting using an antibody specific for phospho-FGFR (Tyr653/654) and FGFR4 (C16) or sandwich ELISA assay.

PARP cleavage and actin (Clone AC-15) were detected by immunoblotting after 48-hour treatment with ASP5878. FRS2, phospho-ERK, ERK, and GAPDH levels in Hep3B2.1-7 tumors were measured by immunoblotting at 6 hours after single oral administration of ASP5878. The following antibodies were purchased: FGFR4 (A10) (sc-136988), FGFR4 (C16) (sc-124), FRS2 (sc-8318), and GAPDH (sc-20357) from Santa Cruz Biotechnology; βKlotho (AF5889) and mouse IgG_1 isotype control (MAB002) from R&D systems; phospho-FGFR (Tyr653/654; #3471), PARP (#9542), ERK (#9102), phospho-ERK (Thr202/Tyr204; #9101), and phospho-FRS2 (Tyr436; #3861) from Cell Signaling Technology; and actin (Clone AC-15, A5441), actin (Clone AC-74, A5316), and FGF19 (HPA036082) from Sigma-Aldrich. The following materials were purchased: cell lysis buffer from Cell Signaling Technology, phosphatase inhibitor cocktail from Thermo Scientific, protease inhibitor cocktail from Roche Diagnostics, and human total FGFR4 ELISA and human phospho-FGFR4 ELISA kits from R&D systems.

2.5 Xenograft models

All animal experimental procedures were approved by the Institutional Animal Care and Use Committee of Astellas Pharma Inc. In addition, Astellas Pharma Inc., Tsukuba Research Center, has accreditation status awarded by The Association for Assessment and Accreditation of Laboratory Animal Care International. Four-week-old male nude mice (CAnN.Cg-Foxn1nu/CrlCrlj [nu/nu]) were obtained from Charles River Japan. Hep3B2.1-7 cells were subcutaneously inoculated into the flank of mice at 3×10^6 cells/0.1 mL (Matrigel:PBS = 1:1)/mouse and allowed to grow. ASP5878 was administered as a once-daily oral dose initiated after confirming tumor growth in each experiment. Tumor volume was determined using the formula length × width^2 × 0.5. Matrigel was purchased from Corning Incorporated (Life Sciences).

2.6 Xenograft models (sorafenib switch)

Hep3B2.1-7 cells were subcutaneously inoculated into the flank of mice at 3×10^6 cells/0.1 mL (Matrigel:PBS = 1:1)/mouse and allowed to grow. After confirming tumor growth, mice were divided into two groups (n = 10 and 20 for vehicle and sorafenib groups, respectively) on day 0 on the basis of tumor volume and body weight. Vehicle (Cremophor EL/ethanol) or sorafenib (10 mg/kg) was administered as a once-daily oral dose from days 0 to 13. On day 14, the vehicle group was further divided into two groups (five per group), and the sorafenib group was further divided into four groups (five per group) on the basis of tumor volume and body weight. Vehicle (Cremophor EL/ethanol or 0.5% MC), sorafenib (10 mg/kg), or ASP5878 (3 mg/kg) was administered as a once-daily dose from days 14 to 52. The other two groups were used for a different research purpose. Tumor volume was determined using the formula length × width^2 × 0.5.

2.7 HCC orthotopic xenograft model

HuH-7–expressing luciferase (HuH-7-Luc) cells were obtained by infecting HuH-7 cells with lentivirus-expressing luciferase in the presence of blasticidin S (10 μg/mL). HuH-7-Luc cells were inoculated into hepatic parenchyma at 3×10^5 cells/0.01 mL (Matrigel 100%)/mouse. One week after

inoculation, the mice were divided into three groups (n = 5 per group) on day 0 on the basis of bioluminescent imaging. Vehicle (Cremophor EL/ethanol or 0.5% MC), sorafenib (30 mg/kg), or ASP5878 (3 mg/kg) was administered as a once-daily oral dose for 91 days. Tumor growth was monitored by *in vivo* bioluminescent imaging of the abdomen after intraperitoneally injecting luciferin using IVIS-Lumina2 (PerkinElmer Inc.). During the study period (181 days), the survival of mice bearing hepatic tumors was recorded. The condition of the mice was monitored daily. The mice were scored as dead if any of the following signs of suffering were observed: cachexia, weakening, and difficulty in moving or eating. Mice that were scored as dead were euthanized.

3. Results

3.1 Kinase inhibition profile of ASP5878

ASP5878 (Figure 1-1A) potently inhibited the tyrosine kinase activities of recombinant FGFR1, 2, 3, and 4. IC_{50} values were 0.47, 0.60, 0.74, and 3.5 nmol/L, respectively (Table 1-1). Kinase selectivity was tested against a panel of 128 human kinases. FGFRs, VEGFR2, and FMS were the kinases that showed more than 50% inhibition by ASP5878 (200 nmol/L). (Table 1-1). In total, 117 kinases showed less than 50% inhibition (Table 1-3).

3.2 FGF19 expression in 20 HCC cell lines and antiproliferative effect of ASP5878.

Previous reports showed that an FGF19 neutralizing antibody has the potential to be effective in *FGF19*-amplified HCC cell lines. To analyze the antiproliferative sensitivity to ASP5878 and its relationship with FGF19 expression in 20 human HCC cell lines (Figure 1- 1B). FGF19 protein expression in these cell lines was measured by Western blotting (Figure 1-1C), HuH-7, Hep3B2.1-7, and JHH-7 cell lines are sensitive to ASP5878, with IC_{50} values of 27, 8.5, and 21 nmol/L, respectively (Table 1-2). FGF19 protein expression was confirmed in HuH-7, Hep3B2.1-7, and JHH-7 but not in other cell lines (Figure 1-1C). Furthermore, the expression of FGFR4- and its co-receptor βKlotho-protein were observed in HuH-7, Hep3B2.1-7, and JHH-7 (Figure 1-1C). HUH-6 Clone 5, SNU-398, Li-7, and HLF were also sensitive to ASP5878 (Figure 1-1B). The growth inhibition rate of HLF was 64% and those of other ASP5878-sensitive cell lines were higher than 95% at 1,000 nmol/L, the highest concentration examined (data not shown). The mechanisms of inhibition are under investigation. Thus, ASP5878 inhibited the cell proliferation of HCC cell lines expressing *FGF19*.

3.3 Effect of ASP5878 on FGFR signaling

To assess how ASP5878 modulate FGFR4 phosphorylation and the downstream signaling pathway, phosphorylation status were analyzed in Hep3B2.1-7 cells treated with ASP5878by Western blotting. FGFR4 phosphorylation was constitutively observed and inhibited by ASP5878 in a concentration-dependent manner (Figure 1-1D). In addition, ASP5878 treatment suppressed phosphorylation of FRS2 with its mobility shift, and ERK phosphorylation (Figure 1-1E). Furthermore, concentration-dependent increases in PARP cleavage, an apoptosis marker, were detected at 48 hours after ASP5878 treatment (Figure 1-1F). The antiproliferative effects of Hep3B2.1-7 (IC_{50} = 8.5 nmol/L) and ASP5878-induced PARP cleavage at 10 nmol/L are comparable and have no gaps (Table 1-2). A similar effect were confirmed in other FGF19-expressign HCC cell lines, HuH-7 and JHH-7 (data not shown). The suppression of phosphorylation and mobility shift of FRS2 were shown by another FGFR inhibitor in several cell lines. These experiments suggest that the FRS2 mobility shift reflects the phosphorylation status of FRS2 through FGFR signaling.

3.4 ASP5878 induces shrinkage of FGF19-expressing HCC xenograft model

The antitumor efficacy of ASP5878 is evaluated in a Hep3B2.1-7 subcutaneous xenograft mouse model. In this model, a once-daily oral administration of ASP5878 induced tumor regression by 9% and 88% at 1 and 3 mg/kg, respectively (Figure 1-2A), without affecting the body weight for 14 days (Figure 1-2B). To assess the pharmacodynamic effects *in vivo*, the inhibitory effect of ASP5878 on the constitutively activated FGFR downstream signals in Hep3B2.1-7 tumors were evaluated. The mobility shift of FRS2 and suppression of ERK phosphorylation in Hep3B2.1-7 tumors were observed following the administration of 1 and 3 mg/kg ASP5878 (Figure 1-2C). Because of difficulty to detect FGFR4 phosphorylation in Hep3B2.1-7 tumors under xenograft conditions, the effect of ASP5878 on FGFR4 phosphorylation were confirmed in an MDA-MB-453 breast cancer xenograft model. MDA-MB-453 harbors FGFR4-Y367C mutation, which elicits constitutive FGFR4 phosphorylation (Roidl et al., 2010). Six hours after the administration of a single dose, ASP5878 induced the suppression of FGFR4 phosphorylation, mobility shift of FRS2, and suppression of ERK phosphorylation (Figure 1-5). This effect was similar to that detected in Hep3B2.1-7 tumors. These data indicated that ASP5878 suppresses FGFR4 downstream signaling through the inhibition of FGFR4 phosphorylation in Hep3B2.1-7 tumors *in vivo*.

3.5 Survival prolongation of ASP5878 in FGF19-expressing HCC orthotopic xenograft model

To further assess the therapeutic efficacy of ASP5878 in another HCC model, an imageable FGF19-expressing HCC orthotopic xenograft model was established. HuH-7-Luc cells were directly inoculated into the livers of mice, and the implanted cells were monitored by bioluminescent imaging of the upper abdominal area (Figure 1-3A). The bioluminescent emissions of vehicle-treated control mice increased during the subsequent 24 days. Moreover, sorafenib was evaluated as standard therapy for surgically unresectable HCC, as a comparator in this model. Although sorafenib dosing had a slight effect that reduced the emission, ASP5878 reduced the emission to approximately one-fourth of the baseline treatment levels by 3 mg/kg administered as a once-daily oral dose for 24 days. The mean bioluminescent emission in the ASP5878-treated group was lower than that in the vehicle-treated group. These results indicate that the ASP5878-treated mice exhibited a lower tumor burden than vehicle- and sorafenib-treated mice. The emission of ASP5878-treated mice reached background levels on day 31. Continuous ASP5878 treatment sustained the emissions at the background level, and no increase was observed by the end of the dosing at day 90 (Figure 1-3A and 1-3B). These data indicate that ASP5878 treatment induced sustained tumor regression without tumor regrowth. To confirm whether ASP5878 treatment regressed the tumor completely, tumor recurrence was monitored after the cessation of ASP5878 treatment from day 91. No bioluminescent emissions increase was observed 90 days after the cessation of administration from day 91 today 181, when the measurement was quitted (Figure 1-3B). These data indicate that ASP5878 induced complete tumor regression at 90 days. Disease-related mortality was also measured (Figure 1-3C). All the vehicle-treated control mice died by day 52, and all the sorafenib-treated mice died by day 90. In contrast, no mice treated with 3 mg/kg ASP5878 died during the 90-day experimental period. The effects on survival were accompanied by changes in the bioluminescent emissions, with vehicle-treated mice

showing increased emission, whereas mice treated with 3 mg/kg ASP5878 showing reduced emissions.

3.6 Antitumor activity of ASP5878 in the Hep3B2.1-7 xenograft model after sorafenib treatment

Sorafenib is the first line standard therapy for unresectable HCC. the anti-tumor effect of ASP5878 after sorafenib treatment was evaluated. According to previous reports, a dose of 10 mg/kg/day sorafenib was orally administered (Cheng et al., 2009; Strumberg et al., 2005). In the experiments, sorafenib administration for 14 days caused 40% tumor growth inhibition in the Hep3B2.1-7 xenograft model. Even after continuous sorafenib treatment, the Hep3B2.1-7 tumor gradually enlarged, and 47% tumor growth inhibition was observed by day 31. In contrast, the switch from sorafenib to ASP5878 on day 14 induced 83% tumor regression on day 52 relative to the tumor size observed on day 14 (Figure 1-4). This indicates the therapeutic potential of ASP5878 for FGF19-overexpressing HCC patients who previously received sorafenib treatment.

4. Discussion

Recent clinical success in molecular-targeted therapies for cancer based on the identification of oncogenic gene alterations and their specific inhibitors is associated with dramatic antitumor effect, reduced side effects, and improved patient survival. The molecular-targeted therapies include Herceptin for *HER2/neu receptor* amplification and overexpression in breast cancer patients (Hudis, 2007), XALKORI for *echinoderm microtubule-associated protein-like 4–anaplastic lymphoma kinase fusion oncogene*-positive non–small-cell lung cancer (Malik et al., 2014), and Tarceva for *EGFR*-mutated non–small cell lung cancer (Pao et al., 2004). Although there have been no driver oncogene-targeted therapies for HCC, recent data suggest that amplified or overexpressed *FGF19* is a "driver oncogene" in HCC and that blockage of the FGF19–FGFR4 axis could be a novel therapeutic approach for *FGF19*-overexpressing HCC (French et al., 2012; Guagnano et al., 2012; Miura et al., 2012; Sawey et al., 2011).

There have been reports on the importance of FGF signaling in the development of various types of cancer, and this explains the interest in the development of FGFR- or FGF-selective inhibitors (Liang et al., 2013). The most clinically advanced agents targeting HCC are mainly *broad*-spectrum kinase inhibitors with VEGFR2 inhibitory activity (Sandhu et al., 2014). The inhibitory activity of such kinase inhibitors on FGFR4 kinase activity is less effective than the inhibitory activity on VEGFR2 (Sandhu et al., 2014). On the other hand, FGFR-selective inhibitors (NPV-BGJ398, AZD4547, and JNJ-42756493) are being developed for the treatment of lung/breast cancer with *FGFR1* gene amplification, gastric cancer with *FGFR2* gene amplification, cholangiocarcinoma with *FGFR2* fusion, and urothelial cancer with *FGFR3* gene alterations but not for HCC (Arkenau H, 2014; Bahleda R, 2014; Sandhu et al., 2014). Recently, two FGFR4-specific kinase inhibitors, BLU9931 and FGF401, have been reported and tested in clinical trials including HCC patients (Hagel et al., 2015; Hierro et al., 2015).

ASP5878 was identified as an FGFR tyrosine kinase inhibitor with potent FGFR4 inhibitory activity. In this study, the preclinical profile of ASP5878 in the FGF19-overexpressing HCC models was demonstrated. ASP5878 is a potent inhibitor of FGFR tyrosine kinases 1, 2, 3, and 4 and is selective against a number of other kinases. Previous studies have shown that cell growth is inhibited by the suppression of FGFR4 expression in *FGF19*-amplified HCC cell lines with an FGFR4 RNAi or FGFR4-neutralizing antibody and FGFR-selective inhibitors (French et al., 2012; Guagnano et al., 2012; Hagel et al., 2015; Hierro et al., 2015; Miura et al., 2012; Sawey et al., 2011). Of the 20 HCC cell lines, abnormal FGF19 protein expression was observed in HuH-7, Hep3B2.1-7, and JHH-7 cell lines. The proliferation of these cell lines was sensitive to ASP5878 and effectively inhibited by ASP5878. Furthermore, ASP5878 treatment potently inhibited cellular FGFR4, FRS2, and ERK activation and induced apoptosis in these HCC cell lines. Although the expression of FGFR4 and βKlotho was also observed in HuH-7, Hep3B2.1-7, and JHH-7 cell lines, some other HCC cell lines such as HepG2 and JHH-5 expressing FGFR4 and βKlotho without abnormal FGF19 expression showed low sensitivity to ASP5878. Thus, using ASP5878, we confirmed that FGF19 overexpression is an oncogenic driver of HCC and a response marker for FGFR4 inhibition in HCC. Immunohistochemical analysis in previous studies demonstrated that FGF19 expression is associated

with recurrence and poor prognosis in HCC patients, and serum FGF19 levels in HCC patients are higher than those in healthy individuals (Hyeon et al., 2013; Miura et al., 2012). These data indicate that the immunohistochemical staining of tumor FGF19 or measurement of serum FGF19 could be a stratification method for FGF19-overexpressing HCC patients. In addition to FGF19-overexpressing HCC, HUH-6 Clone 5, HLF, SNU-398, and Li-7 were sensitive to ASP5878; however, FGF19 expression was not observed. ASP5878 sensitivity of these cell lines could be based on the genetic alteration of other FGF-signaling genes and not the FGF19–FGFR4 axis. For instance, the amplification of *FGF3/FGF4* genes and FGF21 overexpression has recently been observed in an HCC patient (Arao et al., 2013; Yang et al., 2013). A subpopulation of HCC patients with FGFR1 overexpression was thought to be addicted to FGFR1 (Gu et al., 2015). FGFR2 and FGFR3 overexpression contributed to advanced HCC tumorigenesis (Harimoto et al., 2010; Paur et al., 2015; Qiu et al., 2005). For instance, the SNU398 cell line was found to be sensitive to ASP5878 and NPV-BGJ398 but not to the FGFR4-selective inhibitor BLU9931 (Hagel et al., 2015) . FGFR1, 2, and 3, but not FGFR4, could be oncogenic drivers in the SNU398 cell line. We are presently conducting further studies to validate those hypotheses.

Once-daily oral administration of ASP5878 resulted in tumor regression in the Hep3B2.1-7 xenograft model. The antitumor effect was accompanied by the inhibition of FGFR4 and its downstream signaling in Hep3B2.1-7 xenograft tumors. These aspects were supported by the results that oral administration of 3 mg/kg ASP5878 inhibited phospho-FGFR4 and activated FRS2 and ERK in the MDA-MB-453 xenograft model. In the Hep3B2.1-7 xenograft model, the tumor volume decreased after treatment with ASP5878 and was almost at an undetectable level at the end of 3 mg/kg ASP5878 treatment following sorafenib treatment. Sorafenib is the standard first-line systemic drug for advanced HCC, which can extend the duration of survival to 10.7 months in comparison with 7.9 months in the placebo arm (Cheng et al., 2009) . In my experiments, sorafenib induced slight retardation of tumor growth in the HuH-7 orthotopic xenograft and Hep3B2.1-7 xenograft models. On the other hand, oral administration of 3 mg/kg ASP5878 induced tumor regression and downstream signals declined to background levels in the Hep3B2.1-7 xenograft model. Furthermore, the survival was enhanced in association with the potent antitumor effect of ASP5878 in the HuH-7 orthotopic xenograft model. Importantly, no tumor regrowth was observed among the two different models during ASP5878 administration. Furthermore, ASP5878 induced complete tumor regression, which was sustained for at least 90 days after the cessation of ASP5878 treatment in the HuH-7 orthotopic xenograft model. These data indicated that ASP5878 treatment of FGF19-expressing HCC induced sustained complete regression without recurrence

Several FGFR inhibitors are being investigated in clinical trials, but ASP5878 has a different profile than FGFR inhibitors (Hierro et al., 2015). AZD4547 and NPV-BGJ398 show at least 30-fold greater selectivity toward FGFR1–3 than toward FGFR4 (Gavine et al., 2012; Guagnano et al., 2011). These inhibitors are categorized as pan-FGFR1, 2, and 3 inhibitors. It has not been demonstrated that those two inhibitors showed activity in HCC vivo model. In contrast, ASP5878 has potent FGFR4 inhibitory activity. It showed remarkable tumor regression and extended survival in an HCC model *in vivo*, without weight loss. Similar efficacy and tolerability may be achieved in HCC patients; this

hypothesis is currently being evaluated in clinical trials. BLU9931 showed >50-fold greater inhibition of FGFR4 than of FGFR1, 2, and 3 (Hagel et al., 2015). FGF401 has reported to be an FGFR4-selective inhibitor, but the kinase selectivity profile remains unknown (Hierro et al., 2015). Similar to ASP5878, these inhibitors are expected to improve the therapeutic outcome of HCC patients with FGF19 overexpression. The advantage of ASP5878 over FGFR4-selective inhibitors is the ability to provide therapeutic benefit to a subset of patients with HCC whose tumors are driven by FGFR1, 2, or 3. In addition to FGFR4, the overexpression of FGFR1, FGFR2, and FGFR3 contributes to advanced HCC tumorigenesis, metastasis, and poor prognosis (Gu et al., 2015; Harimoto et al., 2010; Paur et al., 2015). In particular, Paur and colleagues observed that FGFR3 and/or FGFR4 expression was elevated in 68% of HCC patients (Paur et al., 2015). Moreover, the amplification of *FGF3/FGF4* genes and FGF21 overexpression has recently been observed in an HCC patient (Arao et al., 2013; Yang et al., 2013). These ligands bind to FGFR1, 2, and/or FGFR3. ASP5878 may be beneficial for these HCC subpopulations. In fact, the SNU398 cell line was sensitive to ASP5878 and BGJ398 but not to BLU9931; SNU398 may be one of the representatives of these HCC subsets. JNJ-42756493 was found to inhibit all members of the FGFR family at the low nanomolar IC_{50} range (Verstraete et al., 2015). This type of compound is categorized as a "pan-FGFR1, 2, 3, and 4 inhibitor," including ASP5878. JNJ-42756493 is currently being evaluated in clinical trials. Hyperphosphatemia has been observed with other FGFR inhibitors (e.g., AZD4547 and JNJ-42756493) and is likely based on the mechanism of action (Arkenau H, 2014; Lin and Desnoyers, 2012). In line with the findings, increased serum phosphate was observed in rodents repeatedly administered with ASP5878 (unpublished data).

In conclusion, using a panel of HCC cell lines *in vitro*, it has been shown that FGF19 protein expression levels predict the antiproliferative sensitivity to the novel and potent FGFR-selective agent ASP5878. ASP5878 induced almost complete tumor regression in association with the pharmacodynamic modulation of FGFR downstream signals in a Hep3B2.1-7 xenograft model. Furthermore, ASP5878 showed complete and sustained tumor regression and extended survival in a HuH-7 orthotopic xenograft model. Our findings demonstrate that ASP5878, a novel FGFR inhibitor with potent FGFR4 inhibitory activity, is expected to improve the therapeutic outcomes of HCC patients with FGF19 overexpression.

5. Tables

Table 1-1. Kinase inhibition profile of ASP5878

Kinase	IC_{50} (nmol/L)	95% confidence interval
FGFR4	3.5	2.1–5.9
FGFR1	0.47	0.28–0.78
FGFR2	0.60	0.36–1.0
FGFR3	0.74	0.3–1.8
FGFR3 (K650E)	1.6	1.3–1.9
FGFR3 (K650M)	4.2	3.1–5.6
VEGFR2	25	19—32
FGFR4 (N535K)	78	26—230
FMS	150	100—220

NOTE: Other TKs, <50% inhibition at 200 nmol/L.

Table 1-2. Antiproliferative effect of ASP5878 in FGF19-expressing HCC cell lines

Cell line	FGF19 status	IC_{50} (nmol/L)	95% confidence interval
Hep3B2.1-7	HCC (overexpression)	8.5	6.7–11
HuH-7	HCC (overexpression)	27	20–37
JHH-7	HCC (overexpression)	21	18–24
JHH-5	HCC (no expression)	410	270–620
PLC/PRF/5	HCC (no expression)	730	660–800

Table 1-3. Inhibitory activity of ASP5878 against 117 kinases

Kinase	% Inhibition ASP5878 200 nmol/L	Kinase	% Inhibition ASP5878 200 nmol/L
ABL	0.0	LCK	0.0
ABL (E255K)	−3.3	LTK	−1.9
ABL (T315I)	11.4	LYNa	0.7
ACK	1.3	LYNb	5.8
ALK	−5.2	MER	−3.1
ALK (F1174L)	−6.5	MET	−10.3
ALK (L1196M)	−10.8	MET (Y1235D)	−9.9
ALK (R1275Q)	0.1	MUSK	−7.8
NPM1-ALK	−0.1	PDGFRα	8.0
ARG	−1.3	PDGFRα (T674I)	16.3
AXL	−3.5	PDGFRα (V561D)	6.9
BLK	5.7	PDGFRβ	2.3
BMX	−4.9	PYK2	−1.2
BRK	−3.2	RET (M918T)	38.4
BTK	−5.0	RON	−11.0
CSK	−0.8	ROS	−3.2
DDR1	−0.4	SRC	−4.8
DDR2	−4.2	SRM	−4.7
EGFR	−8.8	SYK	−6.5
EGFR (d746-750)	−6.2	TEC	−3.1
EGFR (d746-750/T790M)	−6.2	TIE2	7.0
EGFR (L858R)	−6.8	TNK1	−3.4
EGFR (L861Q)	−4.5	TRKA	44.2
EGFR (T790M)	−5.8	TRKB	34.1
EGFR (T790M/L858R)	−6.3	TRKC	33.1
EPHA1	−4.0	TXK	−6.6
EPHA2	−5.5	TYK2	6.9
EPHA3	−8.4	TYRO3	9.6
EPHA4	−3.7	YES	5.9
EPHA5	−6.1	ZAP70	3.2
EPHA6	−3.4	AKT1	−4.3

EPHA7	−1.8	AMPKα1/β1/γ1	−6.2
EPHA8	−9.5	AurA	2.5
EPHB1	−4.7	CaMK4	−0.9
EPHB2	−5.9	CDK2/CycA2	−5.6
EPHB3	−6.3	CHK1	−2.7
EPHB4	−5.5	CK1ε	−3.7
FAK	−12.3	DAPK1	−3.0
FER	−9.9	DYRK1B	−0.9
FES	−5.5	Erk2	1.2
FGFR4 (V550E)	−2.6	GSK3β	−6.4
FGFR4 (V550L)	21.0	HGK	−3.4
FGR	2.5	IKKβ	−6.7
FLT3	−3.0	IRAK4	−8.7
FRK	−9.6	JNK2	−4.4
FYN	−4.5	MAPKAPK2	−3.9
HCK	3.6	MST1	−0.8
HER2	−2.0	NEK2	1.1
HER4	−1.5	p70S6K	−1.5
IGF1R	3.8	PAK2	0.0
INSR	9.6	PBK	−9.3
IRR	26.0	PIM1	−5.1
ITK	−5.7	PKACα	−1.2
JAK1	0.0	PKCα	0.7
JAK2	−4.5	PKD2	−2.1
JAK3	0.2	ROCK1	2.7
KIT (D816V)	−9.9	SGK	−4.6
KIT (V560G)	8.1	TSSK1	−2.9
KIT (V654A)	−0.1		

6. Figures

Figure 1-1

A

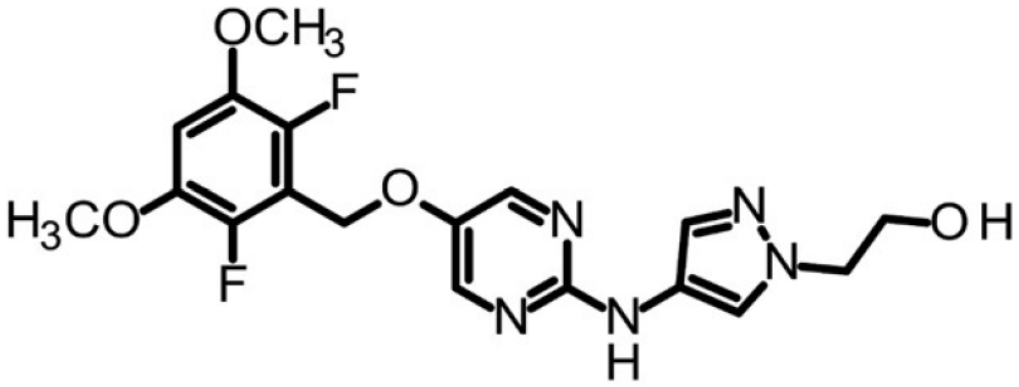

B

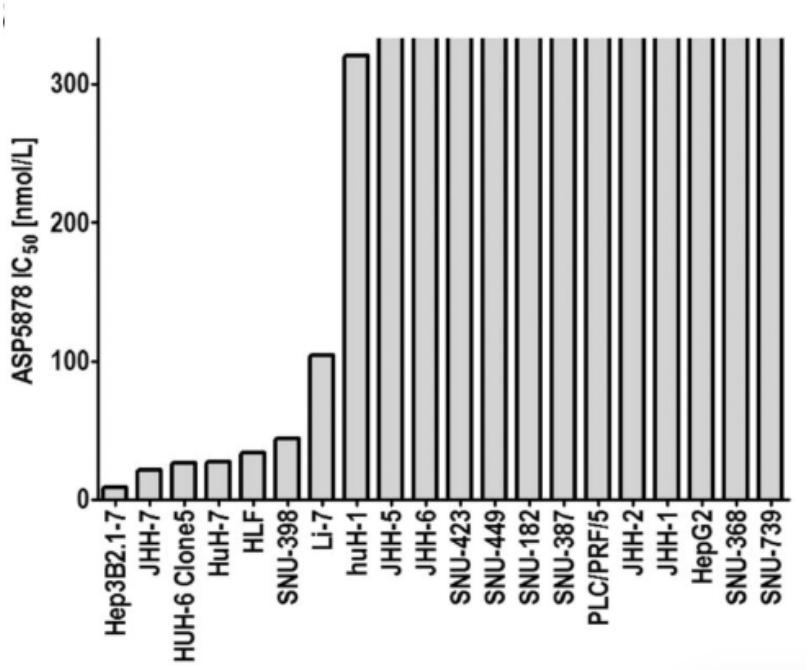

C

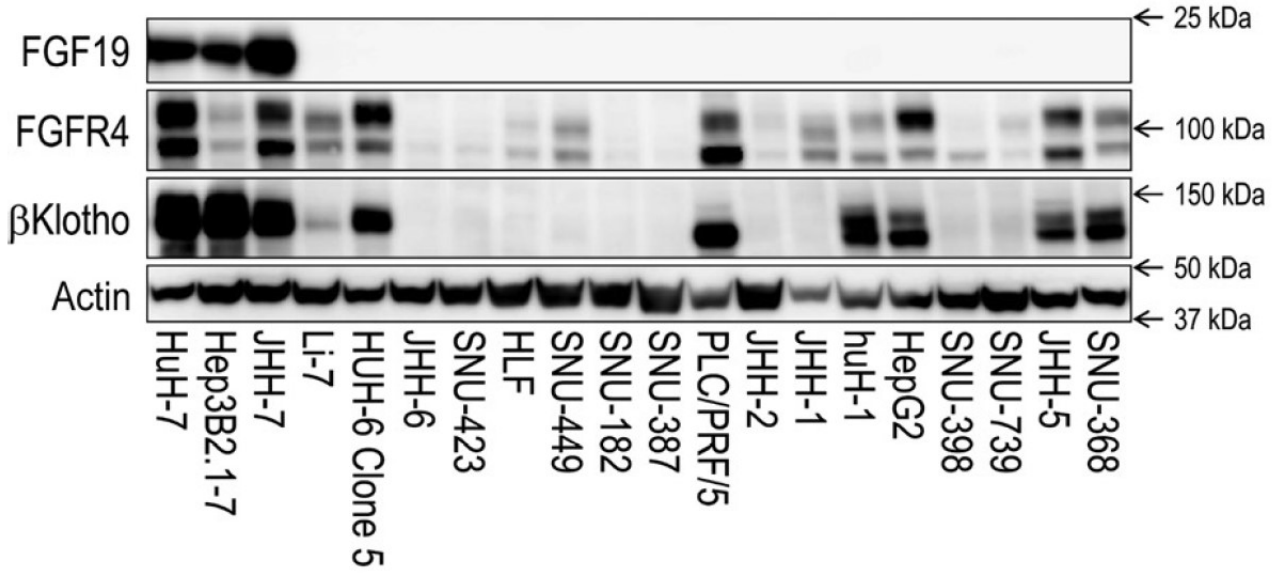
FGF19
FGFR4
βKlotho
Actin
25 kDa
100 kDa
150 kDa
50 kDa
37 kDa
HuH-7
Hep3B2.1-7
JHH-7
Li-7
HUH-6 Clone 5
JHH-6
SNU-423
HLF
SNU-449
SNU-182
SNU-387
PLC/PRF/5
JHH-2
JHH-1
huH-1
HepG2
SNU-398
SNU-739
JHH-5
SNU-368

D

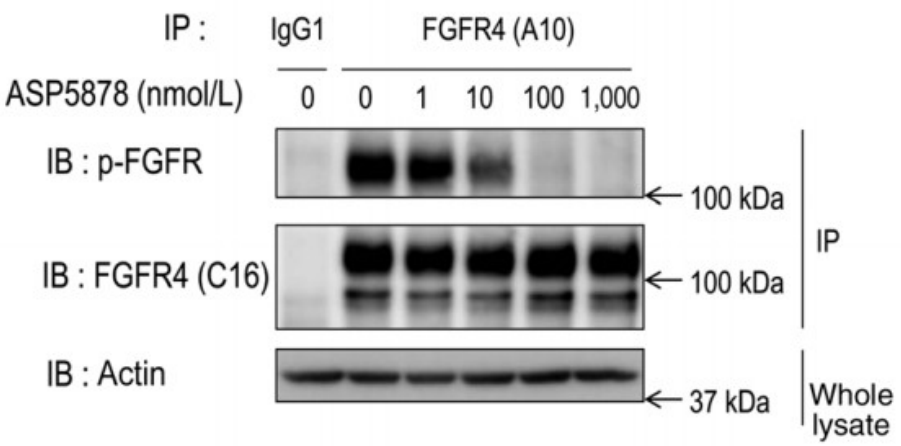
IP :
IgG1
FGFR4 (A10)
ASP5878 (nmol/L)
0
0
1
10
100
1,000
IB : p-FGFR
100 kDa
IB : FGFR4 (C16)
100 kDa
IP
IB : Actin
37 kDa
Whole lysate

E

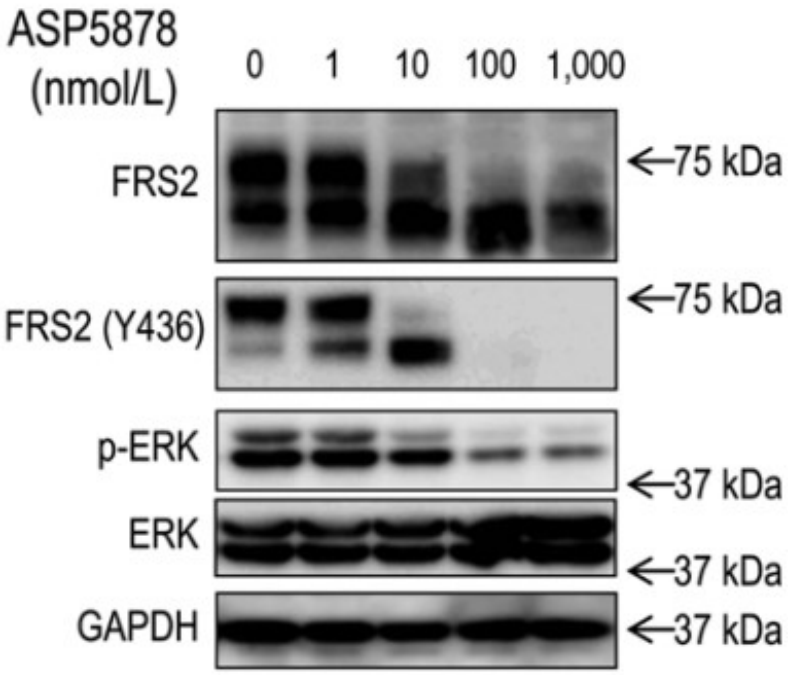

F

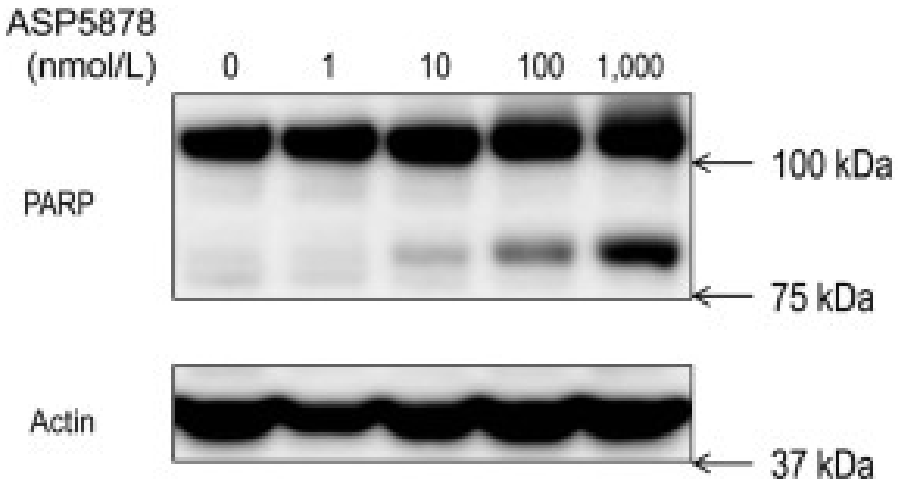

Figure 1-1. Antiproliferative effect of ASP5878 in FGF19-expressing HCC cell lines.

A), Chemical structure of ASP5878, **B)**, In vitro proliferation assay. **C)**, Expression of FGF19, FGFR4, βKlotho, and actin across a panel of 20 human HCC cell lines. **D)**, Inhibition of activated FGFR4 phosphorylation after ASP5878 treatment for 2 hours in Hep3B2.1-7 cells. **E)**, Downstream signals after ASP5878 treatment for 2 hours in Hep3B2.1-7 cells. **F)**, PARP cleavage induced by ASP5878. Hep3B2.1-7 cells were incubated with ASP5878 at the indicated concentration for 48 hours. Each protein was detected by immunoblotting using specific antibodies

Figure 1-2

A

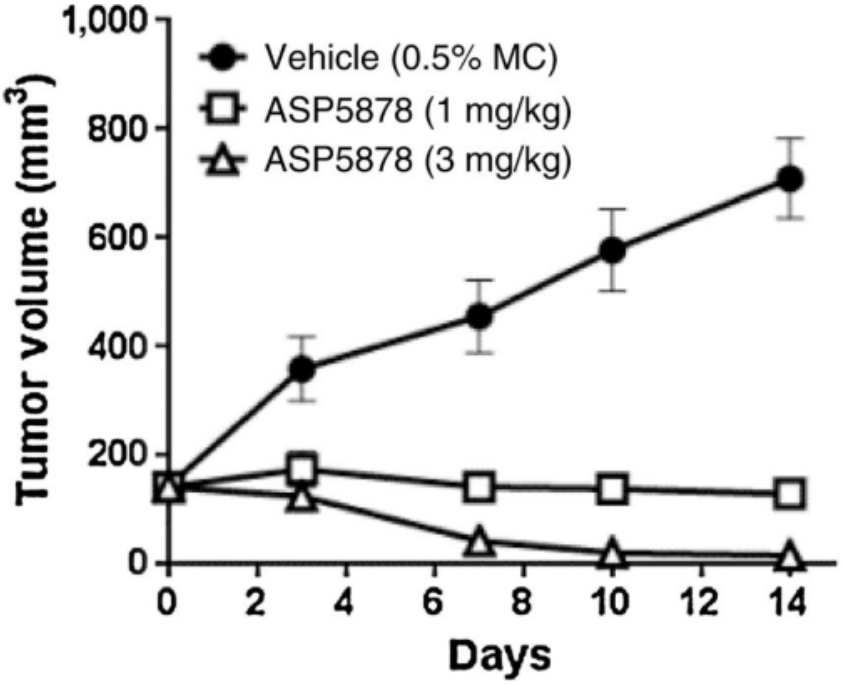

B

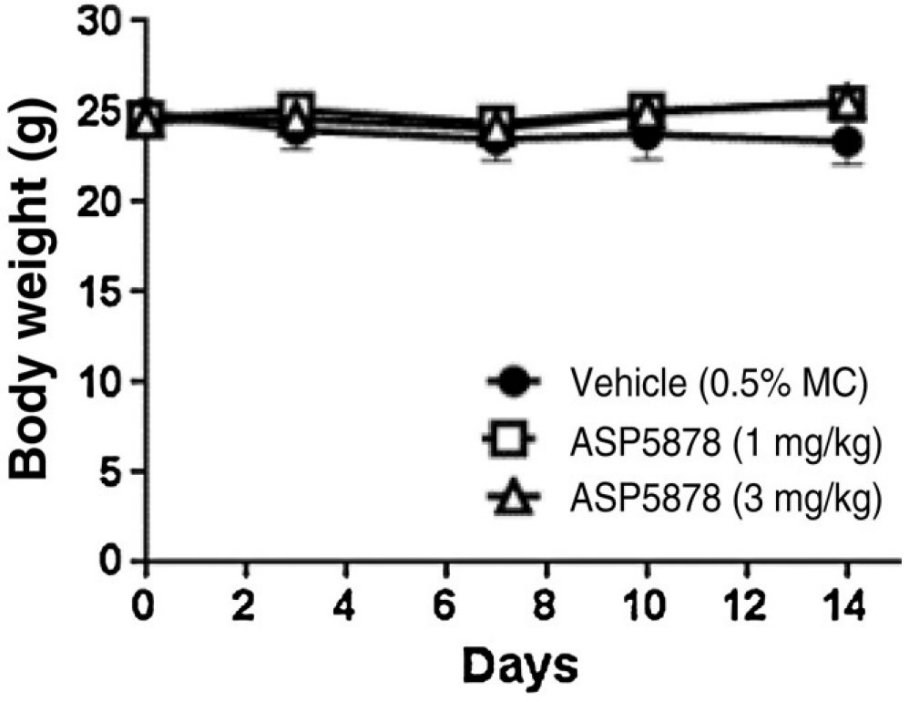

C

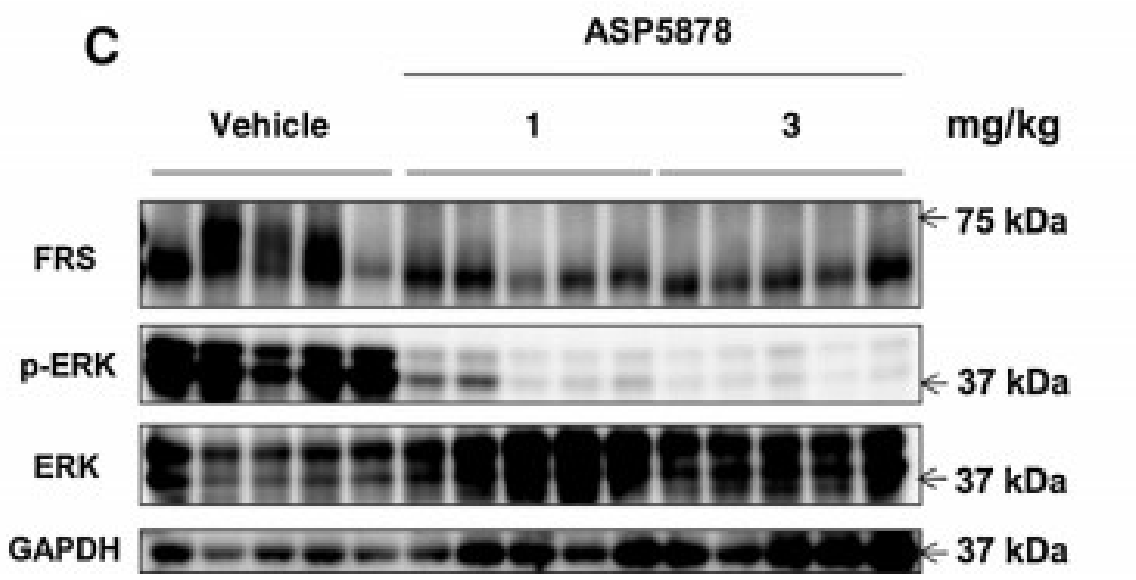

Figure 1-2. ASP5878 treatment leads to tumor regression in FGF19-expressing Hep3B2.1-7 HCC subcutaneous xenograft model.

ASP5878 was orally administrated once daily. Tumor volume **(A)** and body weight **(B)** are expressed as the mean ± SEM ($n = 10$). **C**), Tumor tissues from Hep3B2.1-7 HCC subcutaneous xenograft model treated with 1 and 3 mg/kg ASP5878 were recovered 6 hours after single dosing and analyzed for FRS2 and ERK activation by Western blotting.

Figure 1-3

A

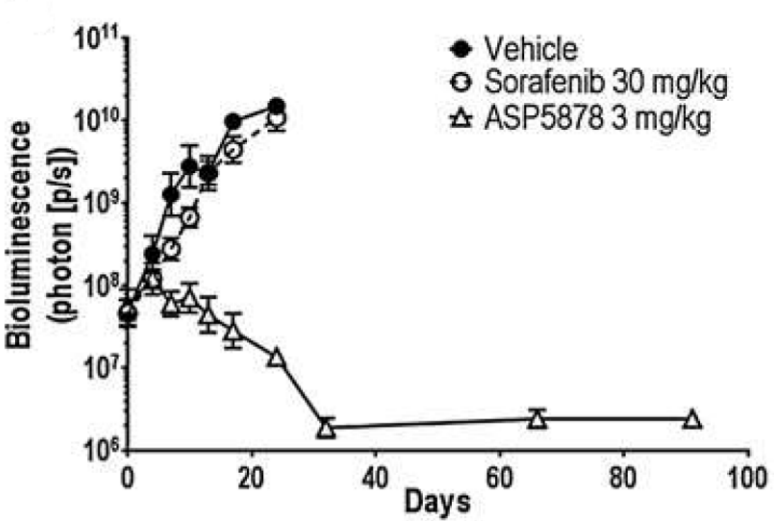
Vehicle
Sorafenib 30 mg/kg
ASP5878 3 mg/kg
Bioluminescence (photon [p/s])
10^{11}
10^{10}
10^{9}
10^{8}
10^{7}
10^{6}
0
20
40
60
80
100
Days

B

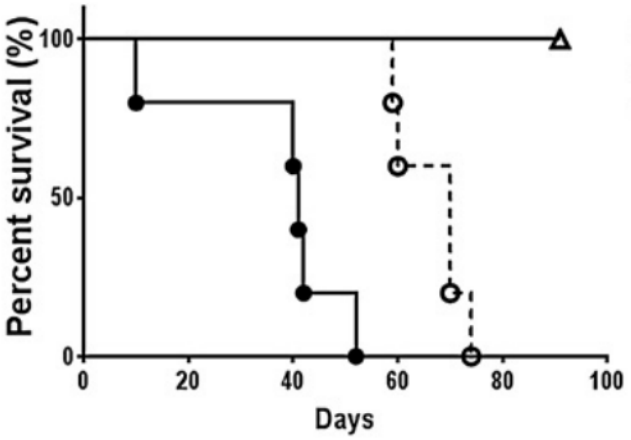
Percent survival (%)
100
50
0
0
20
40
60
80
100
Days

C

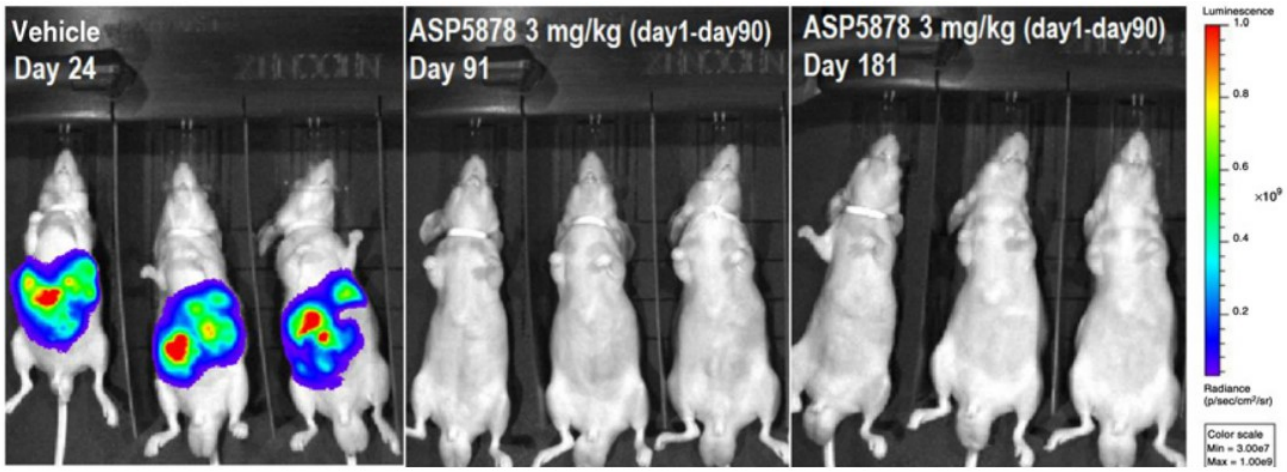

Figure 1-3. ASP5878 treatment leads to tumor regression in FGF19-expressing HuH-7 HCC orthotropic graft model. ↵

HuH-7-Luc cells were directly inoculated into the liver of mice. Vehicle (Cremophor EL/Ethanol), ASP5878 (3 mg/kg), or sorafenib (30 mg/kg) was orally administered once daily at the indicated dose (n = 5). ASP5878 was orally administered once daily from days 1 to 90, and the administration was stopped from day 91 to end of the study, i.e., day 181. **A)**, The implanted cells were monitored using bioluminescent imaging (BLI). Each point represents the mean BLI ± SEM. **B)**, Representative BLI image of each group at the indicated day. **C)**, The survival of mice was monitored daily.↵

Figure 1-4.

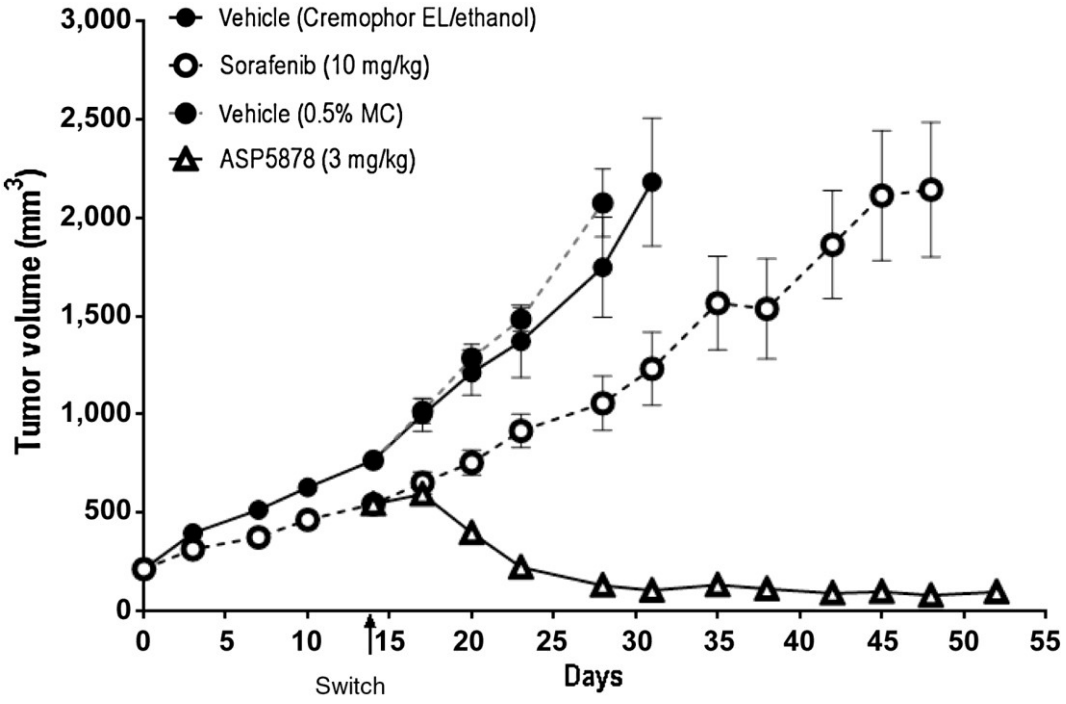

Figure 1-4. Antitumor activity of ASP5878, poorly responsive to sorafenib, in the Hep3B2.1-7 subcutaneous xenograft model

Hep3B2.1-7 cells were subcutaneously inoculated into the flank of mice. Mice were divided into two groups (n = 10 and 20 for vehicle and sorafenib groups, respectively) on day 0 by tumor volume and body weight. Vehicle (Cremophor EL/ethanol) or sorafenib (10 mg/kg) was administered as a once-daily oral dose from days 0 to 13. On day 14, the day of the switch, the vehicle group was further divided into two groups (n = 5 in each group) and the sorafenib group was further divided into four groups (n = 5 in each group) by tumor volume and body weight. Vehicle (Cremophor EL/ethanol or 0.5% MC), sorafenib (10 mg/kg), or ASP5878 (3 mg/kg) was administered as a once-daily dose from days 14 to 52. Tumor volume is expressed as the mean ± SEM.

Figure 1-5.

A

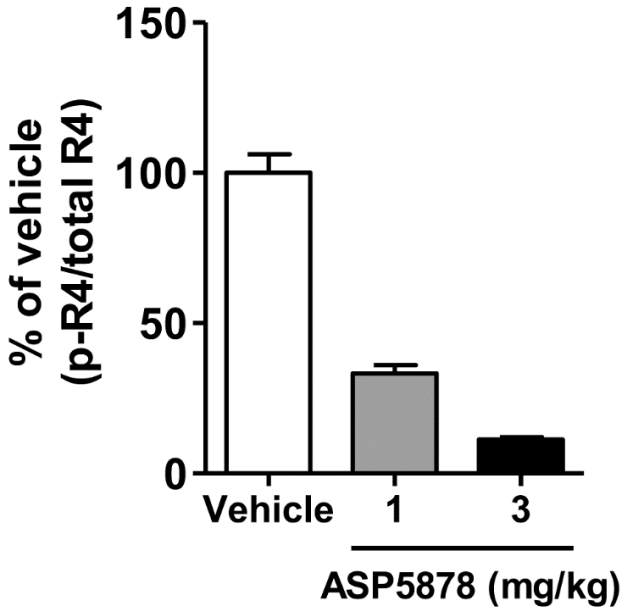

B

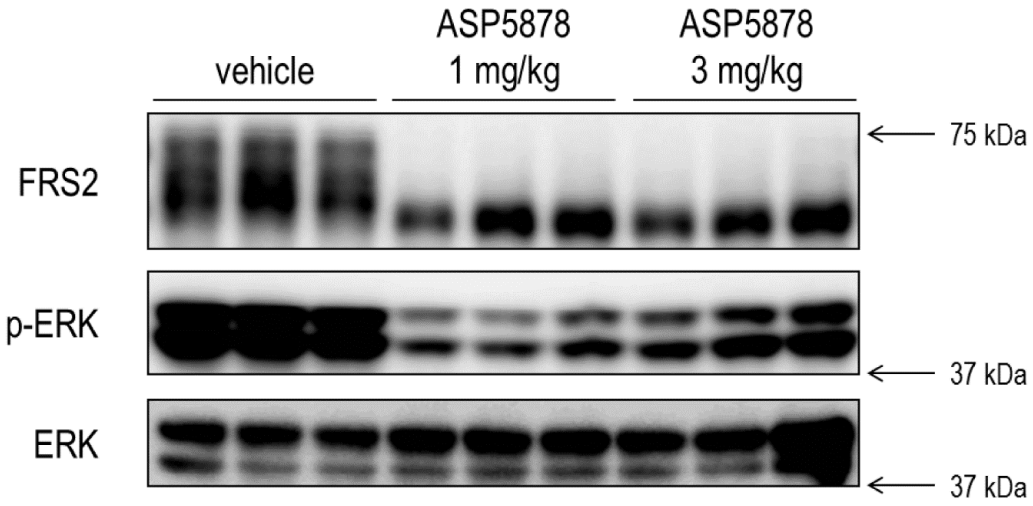

Figure 1-5. ASP5878 inhibited activation of FGFR signals in MDA-MB-453 xenograft model
ASP5878 treatment led to the inhibition of FGFR4 phosphorylation in the MDA-MB-453 subcutaneous xenograft model. Tumor tissues from the MDA-MB-453 xenograft model treated with 1 and 3 mg/kg ASP5878 were recovered 6 h after single dosing and analyzed for **A)** a phosphorylation ratio of FGFR4 by sandwich ELISA and **B)** FRS2 and ERK activation by western blot analysis.

Chapter III: Identification of a novel oncogenic mutation of FGFR4 in gastric cancer

1. Introduction

Gastric cancer is an aggressive cancer with poor prognosis and the fifth-most common cause of cancer-related death worldwide (Liu and Meltzer, 2017). The number of survivors is low because diagnosis is often determined during the late stages when symptoms first appear, which are accompanied by metastasis and chemoresistance (Liu and Meltzer, 2017). Earlier treatment would be aided by detailed knowledge of the molecular characteristics of gastric cancer and the identification of new biomarkers. Most gastric cancers are adenocarcinomas and arise and progress as a result of complex genetic and environmental interactions. The Cancer Genome Atlas (TCGA) identifies mutations that classify gastric cancer into the following subtypes: EBV-positive, microsatellite unstable/instability, genomically stable, and chromosomal instability. The development of trastuzumab targeting ERBB2 is a successful example of translational genetic profiling and precision medicine applied to gastric cancer (Bang et al., 2010). Such novel findings help uncover molecular mechanisms and identify effective therapeutic targets for gastric cancer.

The FGF-FGFR signaling pathway plays a key role in the course of development from early embryogenesis to the formation of various organogenesis and tissue patterning, angiogenesis, and metabolism homeostasis (Beenken and Mohammadi, 2009; Hierro et al., 2015). FGFs and FGFRs are encoded by 18 and four genes, respectively, which are expressed by diverse cell types (Beenken and Mohammadi, 2009; Hierro et al., 2015). Upon ligand binding, FGFRs dimerize, autophosphorylate, and recruit adaptor proteins such as FRS2 (Beenken and Mohammadi, 2009; Hierro et al., 2015). These activate intracellular signaling pathways involved in cell growth, differentiation, and survival. In gastric tissue, FGF10-triggered FGFR2 signaling controls stomach progenitor maintenance, morphogenesis and cellular differentiation during early epithelial growth before differentiation (Nyeng et al., 2007). Approximately 1.2–9% of patients with gastric cancer harbor *FGFR2* amplification associated with increased tumor cell proliferation (Hierro et al., 2017). Oncogenic gene alterations are present in all FGFR family members in human cancers. For example, *FGFR1* amplification occurs in breast, lung, gastric, and bladder cancers (Campbell et al., 2016; Luo et al., 2017; Peifer et al., 2012; Weiss et al., 2010). *FGFR2* amplification, mutations, and fusions occur in breast, liver, uterine, lung, gastric cancer (Tchaicha et al., 2014; Turner et al., 2010; Wu et al., 2013). FGFR3 mutations and fusions occur in bladder and lung cancers (2014; Gao et al., 2018; Wu et al., 2013). In contrast, *FGFR4* is infrequently mutated in cancers. The oncogenic mutations of *FGFR4*, N535K/D and V550E/L, occur in rhabdomyosarcoma (RMS), although other oncogenic mutations are unknown (Taylor et al., 2009). The G388C mutation may be involved in tumor progression, although it is a polymorphism (Morimoto et al., 2003; Ye et al., 2010).

This chapter describes the identification of a novel oncogenic mutation of FGFR4 (G636C) in gastric cancer. It has been demonstrated that G636C is a driver mutation that leads to enhanced sensitivity to a selective FGFR inhibitor. These results provide a rational basis for designing therapies that target FGFR4 in gastric cancer.

2. Materials and methods

2.1 Clinical specimens

RNA specimens (n = 83) purified from primary gastric tumors were obtained from Asterand Bioscience. Written informed consent was obtained from all patients. Patient anonymity was ensured, and the study was approved by the Institutional Review Committees at Astellas Pharma, Inc. (Astellas). Experiments were performed in accordance with Astellas' guidelines.

2.2 Nucleotide sequencing

Total RNAs were reverse-transcribed using SuperScript III reverse transcriptase (Thermo Fisher Scientific). The tyrosine kinase (TK) domain of FGFR4 was amplified from cDNA templates using PCR with the forward primer (5'-CACTGTGGCCGTCAAGATGC-3') and reverse primer (5'-TGCTGGTTTTCTTATAGTAGTCAA-3'). Nucleotide sequencing of PCR products was performed using Big Dye Terminator chemistry (Applied Biosystems) and the forward primer (5'-ATGCTCAAAGACAACGCCTCTGAC-3'). Sequences were analyzed using SeqMan Pro software (DNASTAR, Lasergene). Experiments were carried out in accordance with Astellas' guidelines.

2.3 Plasmids and Cell lines

Human wild-type FGFR4 (wt-R4, NM_213647.1) and G636C-FGFR4 (G636C-R4) were cloned into the pMXs-Puro retroviral vector (Cell Biolabs). NIH/3T3 cells and Ba/F3 cells were obtained from the ATCC and RIKEN Bioresource Center, respectively. Although the cell lines used in this study were not authenticated in our laboratory, they were purchased from providers of authenticated cell lines and stored at early passages in a central cell bank at Astellas. Mycoplasma testing was performed using PCR. The experiments were conducted using low-passage cultures of these stocks. NIH/3T3 cells were cultured in DMEM medium supplemented with 10% heat-inactivated FBS. Ba/F3 cells were maintained in RPMI-1640 medium supplemented with 10% heat-inactivated FBS and mouse IL-3 (10 ng/mL). Wt-R4- or G636C-R4- or mock-infected NIH/3T3 cells and G636C-R4-Ba/F3 cells were generated by Astellas. The pMXs-Puro retroviral vector containing the wt-R4 or G636C-R4 gene or empty vector was transfected into Platinum-E cells using FuGENE HD transfection reagent (Roche Diagnostics) to produce virus stocks. NIH/3T3 and Ba/F3 cells were then infected with viruses with genomes harbouring each FGFR4 construct or control virus. Stable transfectants were obtained and maintained under selection pressure using puromycin at 1.5 μg/mL. G636C-R4-Ba/F3 cells were cultured in RPMI-1640 as described above but without IL-3. Experiments were carried out in accordance with institutional guidelines approved by Astellas.

2.4 In vitro anchorage-independent growth assay

Mock/3T3, wt-R4/3T3 and G636C-R4/3T3 cells (1000 cells per well) were plated in DMEM supplemented with 10% heat-inactivated FBS in 96-well Sumilon Celltight spheroid plates (Sumitomo Bakelite) and then incubated at 37 °C in an atmosphere containing 5% CO2. The number of viable cells was determined using the CellTiter-Glo Luminescent Cell Viability Assay

(Promega) on days 1, 4 and 7. Experiments were carried out in accordance with Astellas' guidelines.

2.5 In vitro growth assay

G636C-R4/BaF cells (1000 cells per well) were plated in RPMI-1640 supplemented with 10% heat-inactivated FBS with or without IL-3 (10 ng/mL) in 96-well plates. G636C-R4/3T3 cells (2000 cells per well) were plated in DMEM supplemented with 10% heat-inactivated FBS in PrimeSurface96U plates (Sumitomo Bakelite). The cells were treated with ASP5878 at 0–10,000 nM (3-fold serial dilutions, 10 concentration points) for 4 or 5 days, and the number of viable cells was determined using the CellTiter-Glo Luminescent Cell Viability Assay (Promega). The IC50 value of ASP5878 was calculated using nonlinear regression analysis with the Sigmoid–Emax model, and geometric mean IC50 values and 95% confidence intervals (CIs) were calculated from three individual experiments. Microsoft Excel (Microsoft) and GraphPad Prism (GraphPad Software) were used for data analysis. Experiments were performed in accordance with Astellas' guidelines.

2.6 Western blotting

NIH/3T3 cells were lysed with cell lysis buffer containing phosphatase and protease inhibitors, and the levels of FGFR4, phospho-FGFR4, phospho-ERK1/2, phospho-AKT and β-actin were determined using immunoblotting. The antibodies were as follows: anti-FGFR4 from Santa Cruz Biotechnology, Inc. (Dallas, TX); and anti-phospho-FGFR (Tyr653/654), anti-phospho-ERK (Thr202/Tyr204), anti-phospho-AKT, anti-β-actin and HRP-conjugated anti-rabbit IgG from Cell Signaling Technology (Danvers, MA). All antibodies were diluted 1/2000 for use. Proteins of interest were visualized by enhanced chemiluminescence using the Western Lightning Plus-ECL (PerkinElmer) and detected with LAS-4000 (GE Healthcare). Cell lysis buffer was purchased from Cell Signaling Technology, phosphatase inhibitor cocktail from Thermo Scientific (Rockford, lL) and protease inhibitor cocktail from Roche Diagnostics (Mannheim, Germany). Experiments were performed in accordance with Astellas' guidelines.

2.7 Structural Analysis and Modelling

The amino acid sequence of the kinase domain of wild-type FGFR4 was obtained from the UniProt database (UniProt ID: P22455, isoform 1). Substituting G636 with Cys generated the mutant G636C-FGFR4. The coordinates of the auto-inhibitory conformation of FGFR4 are registered in the protein database (PDB) (PDB ID: 4TYE) (Lesca et al., 2014). An X-ray structure of the phosphorylated catalytically active form of FGFR4 with ATP or ATP analogues is not available, to our knowledge. Therefore, the coordinates of the active conformation of G636C-FGFR4 were modelled according to the phosphorylated- and ATP analogue-bound active form of FGFR1 (PDB ID: 3GQI) (Bae et al., 2009). The coordinates of 3GQI were used as a template for homology modelling of the active form of FGFR4 using the modelling software MOE (Chemical Computing Group). Phosphate moieties of Y642 and Y643 were added after homology modelling, and energy minimization of the coordinates of these residues was performed to relax the coordinates. Further energy minimization including R635 and G636C was performed, because an Arg residue corresponding to R635 forms hydrogen bonds

with a phosphorylated Tyr residue corresponding to Y643 of other FGFR isoforms (Chen et al., 2007; Chen et al., 2008; Hierro et al., 2017).

The coordinates of ASP5878-bound wild-type FGFR4 were modelled according to the coordinates of wild-type FGFR4 bound to the FGFR kinase inhibitor BLU9931 (PDB ID: 4XCU) (Blundell et al., 1987), whose chemical structure is similar to that of ASP5878. Sequentially substituting or removing atoms and bonds of BLU9931 in 4XCU from the atoms binding to the back of the binding pocket generated the initial coordinates of FGFR4 bound to ASP5878. Repetitive optimization calculations of the coordinates were performed using energy minimization, and the atoms of the proteins were fixed using MOE. Finally, the coordinates of the residues within 4.5 angstroms from ASP5878 were repeatedly optimized until the energies converged. The coordinates of ASP5878-G636C-FGFR4 were introduced using homology modelling by MOE that were based on the coordinates of wild-type ASP5878-FGFR4. During the homology modelling, the coordinates of the atoms were initially assigned according to the template structure and finally optimized to minimize the energy level, which reflected the effect of the mutated residue on the coordinates near the residue as well as those of the binding pocket. To visualise the molecules, hydrogen atoms were added using Protonate3D included in MOE.

2.8 Asp5878

ASP5878 (Astellas Pharma Inc (Asaumi M, 2013)) was synthesized in our laboratory. Experiments were performed in accordance with Astellas' guidelines. ASP5878 was dissolved in dimethyl sulfoxide or 0.5% methylcellulose (MC) for *in vitro* or *in vivo* experiments, respectively.

2.9 Xenograft model

The Institutional Animal Care and Use Committee of Astellas approved the experimental protocols for using animals. Astellas Pharma Inc., Tsukuba Research Center is accredited by the Association for Assessment and Accreditation of Laboratory Animal Care International. Experiments were carried out in accordance with Astellas' guidelines. Four-week-old male nude mice (CAnN.Cg-Foxn1nu/CrlCrlj [nu/nu]) were obtained from Charles River Japan.

2.10 In vivo xenograft study of the tumourigenicity of cells expressing G636C-FGFR4

Mock/3T3, wt-R4/3T3 and G636C-R4/3T3 cells were cultured in DMEM supplemented with 10% heat-inactivated FBS, and 0.1 ml of 3×10^6 cells mixed with Matrigel/PBS ([Matrigel:PBS = 1:1]) was subcutaneously inoculated into the flanks of mice. Tumor volume was calculated as follows: $V = \text{length} \times \text{width}^2 \times 0.5$. Matrigel was purchased from Corning Incorporated (Life Sciences).

2.11 In vivo xenograft study on the antitumor activity of ASP5878

G636C-R4/3T3 cells were subcutaneously inoculated into the flanks of mice (5×10^6 cells/0.1 mL

[matrigel:PBS = 1:1]/mouse). Seven days after inoculation, mice with tumors were divided such that the mean tumor volume was similar among the groups on the first day (day 0) of treatment. ASP5878 (3 mg/kg) was orally administered once daily for 8 days. Tumor diameters were measured using a caliper on days 0, 2, 4, and 7, and tumor volume was determined by calculating the volume of an ellipsoid as follows: length × width^2 × 0.5. Body weight was measured using a standard balance

2.12 Statistical analysis

The values for the mouse xenograft model are expressed as the mean ± SEM. Differences between groups were analyzed using the Student t test. $P < 0.05$ was considered statistically significant. Microsoft Excel (Microsoft) and GraphPad Prism (GraphPad Software) were used for data analysis.

3. Results

3.1. Identification of FGFR4 TK-domain mutations in human gastric cancer

Oncogenic mutations of *FGFR4* occur in RMS, in which FGFR4 is highly expressed (Taylor et al., 2009). High FGFR4 expression correlates with tumor progression and survival in patients with gastric cancer (Ye et al., 2010). Therefore, It has been hypothesized that FGFR4 plays an important role in gastric cancer and that mutations that activate the protein tyrosine kinase activity of FGFR4 promote an aggressive phenotype. Accordingly, activating *FGFR4* mutations was searched by sequencing the tyrosine kinase domain in 83 gastric cancer tissue specimens. A mutation in one sample (St041) at nucleotide position 1906 (NM_213647.1) was identified, which substitutes Gly with Cys at amino acid residue 636 (Figure 2- 1). Comparison with other clinical specimens revealed no clinical diagnostic features or stage that were unique to St041. This mutation is referenced in the Cancer Genome Atlas (TCGA: https://www.cancer.gov/about-nci/organization/ccg/research/structural-genomics/tcga), the Catalogue Of Somatic Mutations In Cancer (COSMIC; http://www.sanger.ac.uk/genetics/CGP/cosmic), dbSNP (http://www.ncbi.nlm.nih.gov/SNP) and the Human Gene Mutation Database (http://www.hgmd.cf.ac.uk/ac/index.php). G636C mutation was identified in oesophagogastric junctional adenocarcinoma and registered in the COSMIC database (COSMIC v89) (Chong et al., 2013). This report did not include experimental analysis (Chong et al., 2013). Further, no human gastric cancer cell lines harbouring the G636C mutation are listed in COSMIC (GRCh38 CELL_LINES v89).

3.2. Structural analysis and modelling of FGFR4-G636C

To investigate whether or not G636C contributes to the activation of FGFR4, multiple x-ray crystallographic structures of FGFR4 deposited in the PDB was searched. G636 is located at a critical position that maintains the auto-inhibitory conformation (PDB code 4TYE) (Lesca et al., 2014) and G636 resides in the activation loop of the FGFR4 TK domain (Figure 2- 2A). Specifically, the residues around G636 form a β-hairpin within an A-loop; moreover, only R635 and G636 reside on the tip of the turn between the two antiparallel β-strands (Figure 2- 2A). Through analysis of the dihedral angles of the backbone atoms around R635 and G636, this structural motif is classified as a β-hairpin type I' conformation, and Gly is the most frequent amino acid residue that forms this conformation (Blundell et al., 1987; Gunasekaran et al., 1997; Lesca et al., 2014; Milner-White and Poet, 1986). In FGFR4, the backbone atoms at A634 and V637 form hydrogen bonds, and R635 and G636 make a sharp turn. The side-chains of L633 and H638 interact via a CH-π bond that may stabilize this conformation.

In contrast, it was unable to identify X-ray structures of phosphorylated catalytically active conformations of FGFR4. Homology modelling of phosphorylated G636C-FGFR4 in a catalytically active conformation indicated that C636 is located near the αC helix and engaged in hydrophobic interactions with V523 and L526 (Figure 2- 2B). Further, C608 is located within 4.5 angstroms from

G636C. Because Cys is more hydrophobic than Gly, this result suggests that G636C strengthens this interaction in the active conformation.

3.3. The G636C mutation promotes autophosphorylation of FGFR4 and phosphorylation of AKT and ERK

Base on the result of structural analysis, , NIH/3T3 cells was transduced with the wild-type human FGFR4 or G636C expression vector or empty vector (wt-R4/3T3, G636C-R4/3T3 and mock/3T3, respectively) to examine whether G636C mutation constitutively activate FGFR4. Western blot analysis showed that wt-R4/3T3 and G636C-R4/3T3 cells expressed comparable levels of FGFR4. Further, the levels of autophosphorylated FGFR4 and phosphorylated AKT and ERK in G636C-R4/3T3 cells were significantly higher compared with those of wt-R4/3T3 cells (Figure 2- 3A). These data indicate that G636C constitutively activates the kinase activity of FGFR4.

3.4. Cells expressing the FGFR4 mutant exhibit a malignant phenotype

Anchorage-independent proliferation analysis was conducted to confirm whether G636C-driven constitutive FGFR4 activation is associated with increased cell proliferation. In spheroid cell cultures, G636C-R4/3T3 underwent anchorage-independent proliferation at a significantly higher rate compared with that of wild-type FGFR4 (Figure 2-3B). Consistent with these findings, subcutaneous injection of G636C-R4/3T3 cells into nude mice generated tumors with significantly larger volumes compared with those generated by wt-R4/3T3 cells (Figure 2-3C). Furthermore, ectopic expression of G636C-FGFR4 conferred IL-3-independent survival and proliferation of Ba/F3 cells, although Ba/F3 cell cannot survive without IL-3 (Kong et al., 2017). Together, these data strongly support the conclusion that the G636C mutation converted FGFR4 into an oncoprotein.

3.5. Antiproliferative effect of FGFR inhibitor on the cells expressing FGFR4-G636C

These results predict the activation of an oncogenic signaling pathway by *FGFR4-G636C*. To support this prediction, G636C-R4/BaF3 and G636C-R4/3T3 cells were treated with the selective FGFR inhibitor ASP5878 (Futami et al., 2017; Kikuchi et al., 2017). G636C-R4/BaF3 cells were sensitive to ASP5878 (IC_{50}, 34.4 nmol/L [95% CI: 24.6–48.2]) in the absence of IL-3 (Figure 2- 4A(a)). Specifically, in the presence of IL-3, the cells were approximately >10–fold less sensitive to ASP5878 (IC_{50} values > 370 nmol/L). In addition, G636C-R4/3T3 cells were sensitive to ASP5878 (IC_{50}, 15.6 nmol/L [95% CI: 13.4–18.1]) (Figure 2- 4A(b)). This effect on cell growth was comparable to those of other ASP5878-sensitive cell lines, which are dependent on FGFR4 signaling (Futami et al., 2017; Kikuchi et al., 2017). The anti-tumor activity of ASP5878 was evaluated in a mouse subcutaneous xenograft model employing G636C-R4/3T3 cells. In this model, once-daily oral administration of ASP5878 (3 mg/kg) inhibited tumor growth by 60% (Figure 2- 4B) without body weight loss (data not shown). Three-dimensional structural modelling of wild-type and G636C-FGFR4 bound to ASP5878 indicated that the G636C mutation had no significant effect on binding ASP5878 compared with that of wild-type (Figure 2- 4C). These data indicate that G636C-FGFR4 may serve as a target

for FGFR inhibitors now under evaluation in clinical trials (Hagel et al., 2015; Hierro et al., 2015; Sandhu et al., 2014).

4. Discussion

Recent success in molecularly-targeted therapies for cancer was made possible, in part, by identification of oncogenic gene alterations (Bang et al., 2010; Malik et al., 2014; Pao et al., 2004). These discoveries led to the development of specific inhibitors having efficacious anti-tumor activities and reduced adverse effects compared to standard cytotoxic drugs. Examples include erlotinib and crizotinib, which are specific for mutant EGFRs and ALK/ROS-driven lung cancers, respectively (Bang et al., 2010; Malik et al., 2014; Pao et al., 2004). Although the number of therapies targeted to driver oncogenes of gastric cancer is limited, a humanized monoclonal antibody against HER2 (trastuzumab) was approved by FDA for the treatment of patients with metastatic gastric cancer that overexpress HER2 (Bang et al., 2010; Liu and Meltzer, 2017). Moreover, nine selective FGFR inhibitors are now in development for the treatment for gastric cancer with *FGFR2* amplification (Hierro et al., 2017).Here, a novel oncogenic mutation (G636C) of *FGFR4* was identified in a primary gastric cancer. Computational analysis shows that G636C activated FGFR4 by disrupting the auto-inhibitory conformation and stabilizing the catalytically active conformation of its A-loop (Figure 2- 2). Functional analysis showed that NIH/3T3 fibroblasts ectopically expressing G636C-FGFR4 exhibited a malignant phenotype (Figure 2-3) and that G636C acted as a driver mutation that led to enhanced sensitivity to the FGFR inhibitor ASP5878 (Figure 2-4). The sensitivity of G636C-FGFR4-transformed Ba/F3 cells and NIH/3T3 cells to ASP5878 was comparable to that of other ASP5878-sensitive cell lines (Hep3B2.1-7, HuH-7, and JHH-7), which are dependent on signaling through the FGFR4(Futami et al., 2017; Kikuchi et al., 2017; Turner et al., 2010). Once-daily oral administration of ASP5878 significantly inhibited the growth of tumors in mice engrafted with G636C-FGFR4/3T3 cells (Figure 2-4).

G636C-FGFR4 was identified in only one of 83 gastric tumor specimens. In the absence of studies of larger numbers of gastric tumors from diverse sources, this finding indicates that G636C-FGFR4 is a minor mutation in gastric cancer. G636C-FGFR4 occurs in oesophagogastric junctional adenocarcinoma (Chong et al., 2013). Further, mutations corresponding to G636-FGFR4 include D647N-FGFR1 in lung cancer, D650H-FGFR2 in stomach cancer, D650Y-FGFR2 in endometrial cancer and D641N-FGFR3 in bladder cancer (Jeske et al., 2017; Kakiuchi et al., 2014; Katoh, 2019; Lott et al., 2009). In particular, the tyrosine kinase activity of FGFR3-D641N is increased compared with that of the wild-type isoform (Patani et al., 2016). Analysis by COSIC using Hidden Markov Models (FATHMM) software predicted that these mutations are pathogenic (FATHMM score >0.95). Although further investigation is required to confirm the oncogenicity of these mutations, these observations are suggesting that G636C-FGFR4 and its corresponding mutations in other members of the FGFR family may serve as common therapeutic targets of pan-FGFR inhibitors across tumor type. One of the similar cases, the FDA approved a TRK inhibitor for adult and paediatric patients with cancers that harbour oncogenic *NTRK* fusions involving *NTRK1*, *NTRK2* or *NTRK3*, which are present at low frequencies (commonly <1%) in diverse tumor types (Cocco et al., 2018).

The FGFR-specific inhibitors NPV-BGJ398, AZD4547 and JNJ-42756493 are under development for treating lung and breast cancers with *FGFR1* amplification, gastric cancer

with *FGFR2* amplification, cholangiocarcinomas with an *FGFR2* fusion, and urothelial cancers with *FGFR3* alterations (Sandhu et al., 2014). The FGFR4-specific kinase inhibitors BLU9931 and FGF401 are now in clinical trials that include patients with HCC (Hagel et al., 2015; Hierro et al., 2015). The development of these FGFR inhibitors may provide effective therapies for G636C-positive gastric cancer. For example, JNJ-42756493, a potent inhibitor of the tyrosine kinase activities of the four FGFR family members, may be beneficial for treating gastric cancer with *FGFR2* amplification and those that harbour the G636C-FGFR4 mutation (Perera et al., 2017).

FGFRs exist in an equilibrium between active and inactive conformations, and gain-of-function mutations shift the equilibrium to the active conformation (Chen et al., 2017). Therefore, we evaluated potential mechanisms that may explain how G636C increases the kinase activity of FGFR4 (Figure 2-5) as follows: (1) destabilization of the inactive conformation and (2) stabilization of the active conformation, which shift the equilibrium to the active conformation. We first focused on the destabilization of the inactive conformation, because we found that G636 forms a two-residue β-hairpin type-I' conformation in the auto-inhibitory conformation (Figure 2-2A). Moreover, Gly resides at this position in most type-I' β-hairpin structures (Blundell et al., 1987; Gunasekaran et al., 1997; Lesca et al., 2014; Milner-White and Poet, 1986), suggesting that FGFR4-G636C likely disrupts this β-hairpin structure. Such a conformational change may increase the dynamics of the activation loop and increase the probability of exposing Y642 and Y643 to solvent. In the auto-inhibitory conformation, Y642 and Y643 prevent the insertion of ATP into the binding pocket, leading to inhibition of kinase activity (Lesca et al., 2014). Moreover, the phosphorylation of the two tyrosine residues is required to activate the FGFR4 kinase (Wang et al., 2008). Therefore, G636C may increase the exposure of the two Tyr residues to solvent, increasing the probability that ATP binds the pocket and the two tyrosine residues are phosphorylated.

It has been considered that G636C increases the population of active conformers of FGFR4 via stabilization of the active conformation. Because, the active conformation of FGFR4 in the PDB are not registered,the 3D structure of phosphorylated G636C-FGFR4 was precited and the interaction network surrounding the mutated residue was investigated in Figure 2-2B. The results reveal that C636 is most likely positioned near V523, L526 and C608. V523 and L526 reside in the αC helix, and C608 in the β-strand contributes to the formation of the β-sheet within a region of the A-loop. Analyses of X-ray structures and NMR data of mutated FGFRs indicate that critical common mechanisms for the activation of FGFR kinase activity are as follows: "molecular brake", "DFG-latch", "A-loop plug" and "αC tether" (Chen et al., 2017).

The mechanism of the "αC tether" involves a stabilization of the active conformation through interaction between the activation loop and a catalytically critical αC helix. This mechanism was demonstrated using variants of FGFR2-D650, which interact with M537 and M540 in the αC helix in the active conformation (Chen et al., 2008). The study found that the more hydrophobic residues D650A, D650L, D650V and D650I increased FGFR2 kinase activity by 3-fold to 19-fold, whereas D650G, which lacks a side-chain that interacts with M537 and M540, decreases kinase activity (Chen et al., 2017). Further, analysis of the variants M537 and M540 revealed a correlation between hydrophobicity at these positions and kinase activity (Chen et al., 2017). Accordingly, D650

contributes to kinase activation by stabilizing the active conformation through formation of a hydrophobic interaction with the catalytically important αC helix (Chen et al., 2017). Moreover, D650, M537 and M540 of FGFR2 correspond to G636, V523 and L526 of FGFR4, respectively.

Therefore, the present modelling of the active form of FGFR4 is consistent with these observations, suggesting that the effect of the G636C mutation on kinase activity is explained by the "αC tether" mechanism. this model predicts that G636C similarly interacts with V523 and L526 in the αC helix, possibly strengthening the hydrophobic interaction compared with that of wild-type G636. However, in the FGFR3-D641 variants, equivalent to D650 in FGFR2, D641N and D641G increase kinase activity (Patani et al., 2016). This observation suggests that another mechanism activates the kinase. Further, our results indicate that FGFR4-C608 resides close to G636C, suggesting that G636C forms a disulfide bond with C608 to stabilize the active conformation. Further studies are required to reveal the mechanism of the effect of this mutation on the kinase activities of FGFRs. Moreover, our findings indicate that FGFR kinase inhibitors such as ASP5878 may serve as therapeutic agents for gastric cancer.

5. Figures

Figure 2-1.

A

sample No	Nucleotide NM_213647.1	Protein NP_002002.3	site	Clinical Diagnosis (Specimen)	AJCC/UICC Stage	AJCC/UICC Stage Group
St041	G1906T	G636C	Kinase domain	Adenocarcinoma	T4N2M0	IV

B

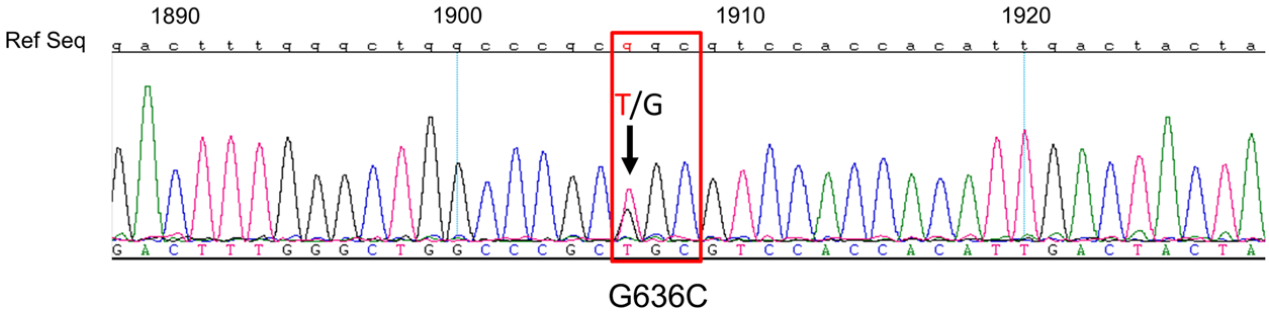

Figure 2-1. FGFR4 TK domain mutations in gastric cancer.

(**A**) Site of mutation in the FGFR4 TK domain identified in a gastric cancer tissue specimen (n = 83).
(**B**) Missense mutation in codon 636 (GGC –> TGC).

Figure 2-2.

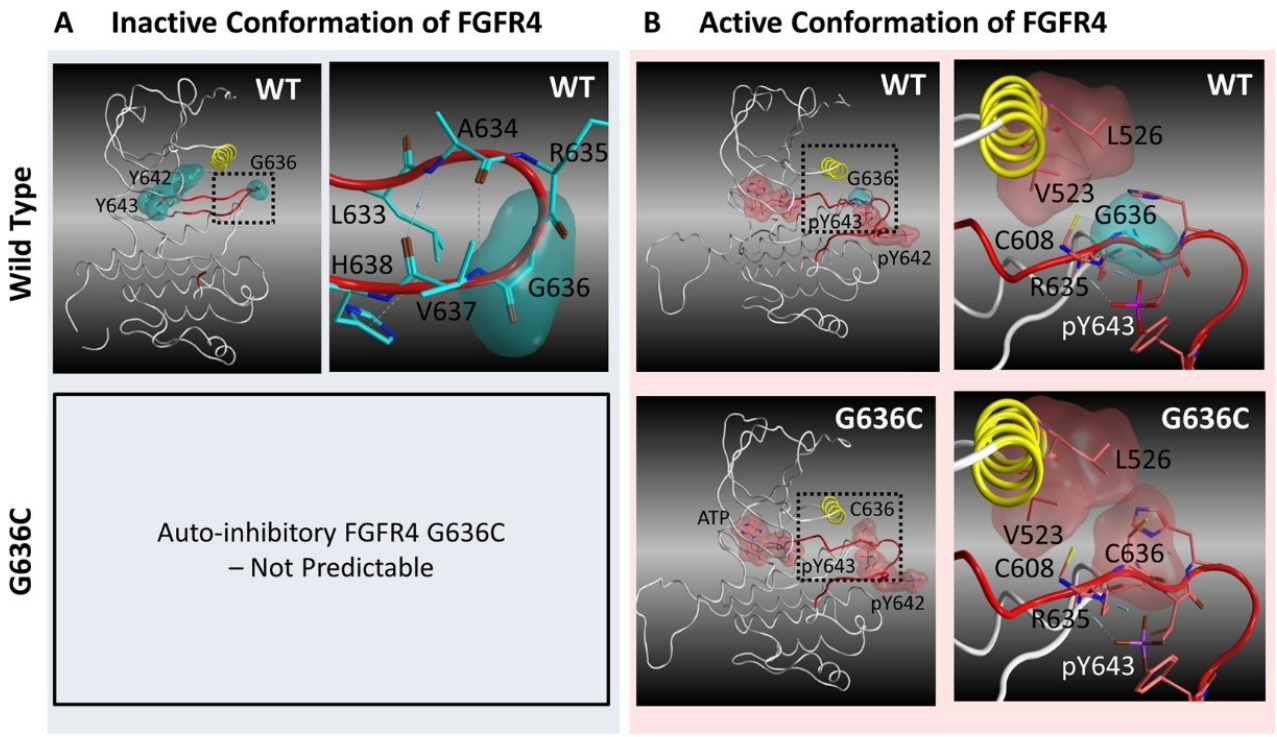

Figure 2-2. Three-dimensional structural models of catalytically inactive and active FGFR4.

(**A**) X-ray structure of the kinase domain of FGFR4 in the auto-inhibitory conformation (PDB code: 4TYE). The αC helix and A-loop are yellow and red, respectively. Blue and yellow dotted lines represent hydrogen bonds and the CH-π bond, respectively. The upper left panel shows an overview of the kinase domain, and the upper right panel shows the amino acid resides within 4.5 angstroms from G636. (**B**) Predicted 3D structure of the catalytically active conformation kinase domain. The left panels show overviews of the kinase domain, and the right panels show the amino acid resides within 4.5 angstroms from G636 or C636.

Figure 2-3.

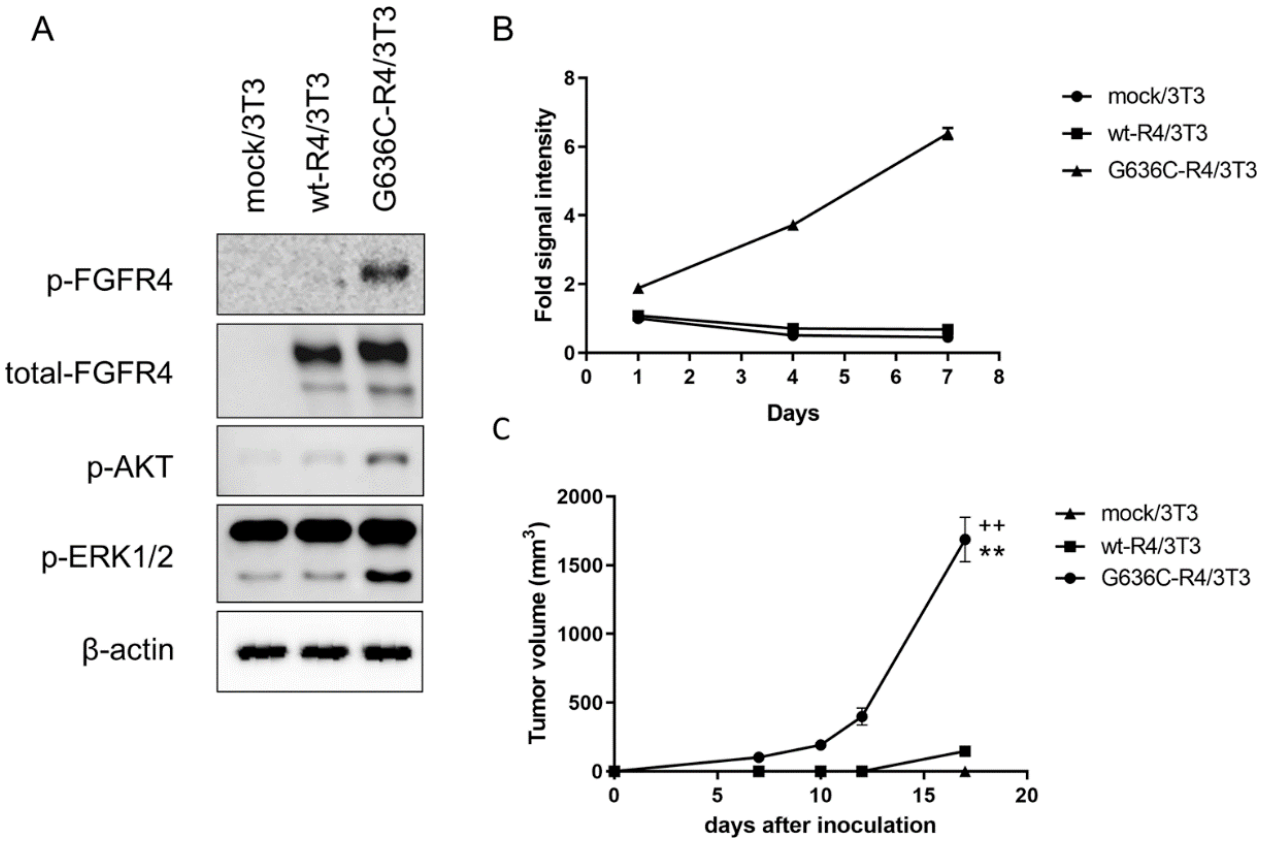

Figure 2-3. G636C-FGFR4 mutations transform 3T3 cells

(**A**) Expression and phosphorylation of G636C-FGFR4 and downstream signaling molecules. The blots cropped from different parts of gels are shown separately, indicated by the black frames. (**B**) Anchorage-independent growth of G636C-R4/3T3 cells. Experiment was performed in triplicate, and data are shown as mean ± SD. (**C**) Tumor growth after subcutaneous injection into mice of G636C-R4/3T3 cells. Data are shown as the mean ± SEM (n = 5). Tumor volumes on day 17 were compared between G636C-R4/3T3 group and the mock/3T3 group (**$P < 0.0001$ Student *t* test), and between G636C-R4/3T3 group and the wt-R4/3T3 group ($^{++}P < 0.0001$ Student *t* test).

Figure 2-4.

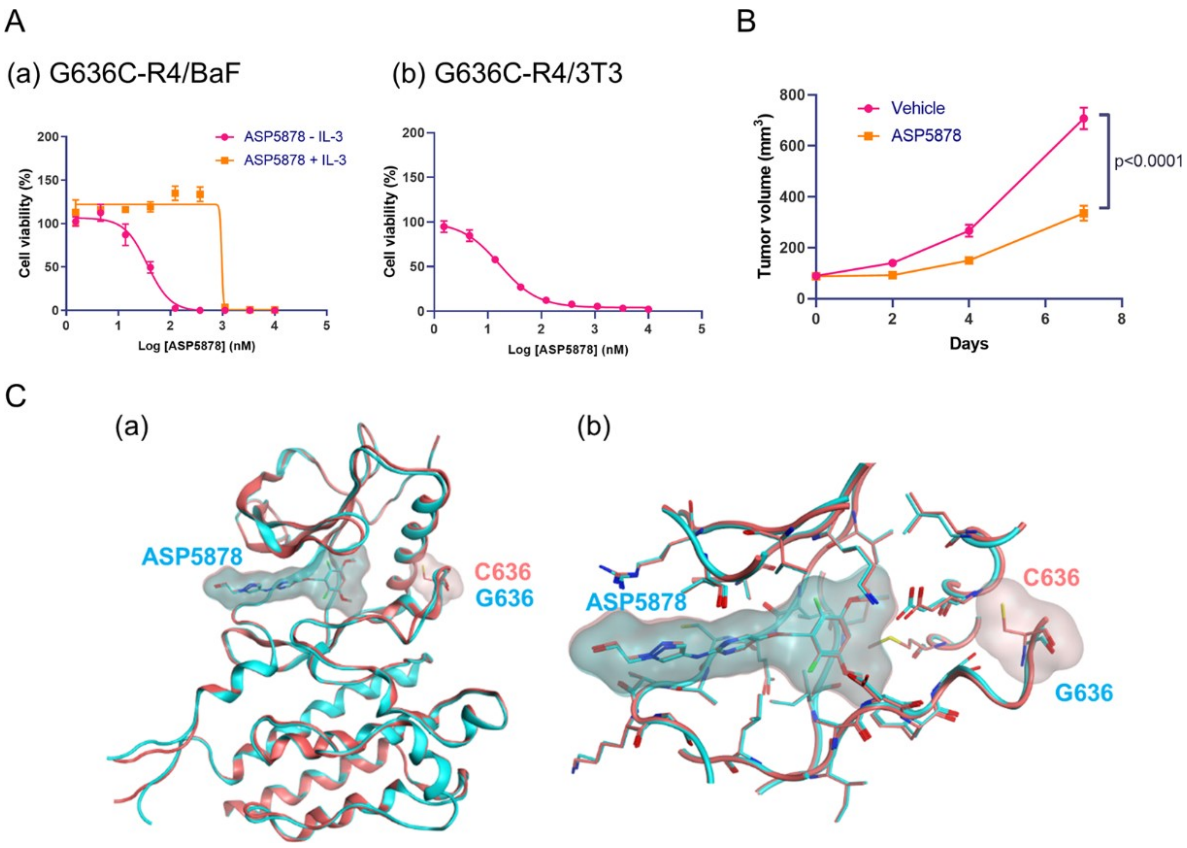

Figure 2-4. Antiproliferative effect of an FGFR inhibitor and 3D structures of FGFR4

(**A**) Antiproliferative effect of ASP5878 on (a) G636C-FGFR4/BaF3 and (b) G636C-FGFR4/3T3 cells. Three independent experiments were performed in triplicate, and representative data are shown as the mean ± SD. Geometric mean IC_{50} values and 95% confidence intervals (CIs) were determined from three independent experiments. (**B**) Mice engrafted with G636C-R4/3T3 cells were orally administered ASP5878 (3 mg/kg, once daily). Tumor volumes were measured, and data are shown as the mean ± SEM (n = 5). Tumor volumes on day 7 were compared between the ASP5878-treated and vehicle control groups (Student *t* test). (**C**) 3D models of FGFR4 wild-type and G636C with ASP5878. (a) Overview of 3D models of the kinase domain of FGFR4 (cyan, wild-type; pink, G636C). The heavy atoms of ASP5878, G636 or C636 are represented as sticks. (b) Close-up of the binding site of ASP5878.

Figure 2-5.

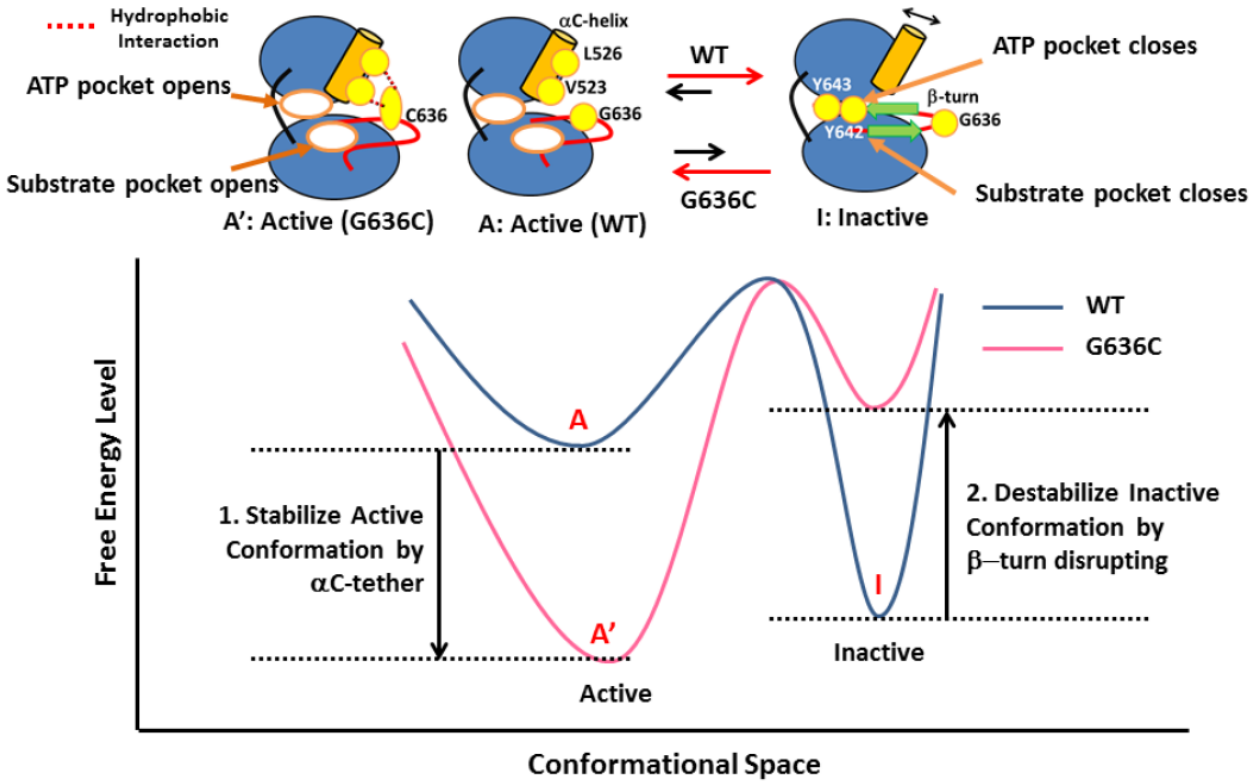

Figure 2-5 Effects of the FGFR4 G636C mutation on the equilibrium between active and inactive conformations.

The kinase domain of FGFR4 is in equilibrium between active and inactive conformations. The probability of the formation of these conformations depends on the free energy level. The lower the free energy of a conformation, the higher its probability. The G636C mutation shifts the equilibrium to the active conformation through the following effects: (1) stabilization and lowering the free energy level of the active conformation through hydrophobic interactions among C636, V523, and L526 (αC-tether), (2) destabilization and increasing the free energy of the inactive conformation by disrupting the β-turn.

General Discussion

Cancer is one of the leading causes of death globally, but recent researches have demonstrated the effectiveness of molecular-targeted therapy based on the identification of oncogenic gene alterations and their specific inhibitors. Molecular-targeted therapy is associated with dramatic antitumor effects, reduced side effects, and improved patient survival.

In chapter II, ASP5878, was identified as a novel FGFR inhibitor and investigated its pharmacological profile and its potential therapeutic efficacy was demonstrated in FGF19-expressing HCC aggressive cancer with poor prognosis. ASP5878 is a novel inhibitor of FGFR1, 2, 3, and 4. It inhibits FGFR4 kinase activity with an IC50 of 3.5 nmol/L (Table 1-1). ASP5878 potently suppressed the growth of the FGF19–expressing HCC cell lines Hep3B2.1-7, HuH-7, and JHH-7 (Table 1-2, Figure 1-1B, 1C). In the Hep3B2.1-7 cell line, ASP5878 inhibited the phosphorylation of FGFR4 and its downstream signaling molecules as well as induced apoptosis (Figure 1-1D, E, F). Oral administration of ASP5878 at 3 mg/kg induced sustained tumor regression in a subcutaneous xenograft mouse model using Hep3B2.1-7 (Figure 1-2A). In HuH-7, an orthotopic xenograft mouse model, ASP5878 induced complete tumor regression (Figure 1-3A) and dramatically extended the survival of the mice (Figure 1-3B, C). These results suggest that ASP5878 is a potentially effective therapeutic agent for HCC patients with tumors expressing FGF19 and that expression of FGF19 in liver could be a potential biomarker to identify the FGFR inhibitor responsive HCC patients.

In chapter III, a novel oncogenic mutation (G636C) of *FGFR4* was identified in a primary gastric cancer (Figure 2-1). Computational analysis showed that G636C activated FGFR4 by disrupting the auto-inhibitory conformation and stabilizing the catalytically active conformation of its A-loop (Figure 2-2). Functional analysis showed that NIH/3T3 fibroblasts ectopically expressing G636C-FGFR4 exhibited a malignant phenotype (Figure 2-3) and that G636C acted as a driver mutation that led to enhanced sensitivity to the FGFR inhibitor ASP5878 (Figure 2-4). The sensitivity of G636C-FGFR4-transformed Ba/F3 cells and NIH/3T3 cells to ASP5878 was comparable to that of other ASP5878-sensitive cell lines (Hep3B2.1-7, HuH-7, and JHH-7), which are dependent on signaling through the FGFR4. Once-daily oral administration of ASP5878 significantly inhibited the growth of tumors in mice engrafted with G636C-FGFR4/3T3 cells (Figure 2-4). These results indicate that FGFR kinase inhibitors such as ASP5878 may serve as therapeutic agents for G636C-FGFR4 positive gastric cancer.

Phase I clinical trial of ASP5878 investigated safety, tolerability, and antitumor effect of single and multiple oral doses of ASP5878 in patients with solid tumors. The safety profile of ASP5878 was similar to those reported for other FGFR inhibitors including BGJ398, JNJ-42756493, and AZD4547, hyperphosphatemia was the most common adverse events. FGFRs are widely expressed in normal tissues and have a key role in development and physiology, especially the phosphate and vitamin D homeostasis. Preclinical models with highly potent selective FGFR inhibitors have caused hyperphosphatemia-mediated tissue calcification owing to blockade of FGF23 release from bone and its signal in the kidney (Brown et al., 2005). Increase in serum FGF23, phosphate, and vitamin D

levels are potential biomarkers for effective FGFR inhibition. In early clinical trials with FGFR inhibitors, development of hyperphosphatemia as a class-specific toxicity may help in the definition of an optimal biological dose (Dienstmann et al., 2011). ASP5878 was well tolerated with manageable toxicities including hyperphosphatemia, such as prophylactic use of phosphate-binding agents and low-phosphate dieting (Yamamoto et al., 2019). FGFR4 selective inhibition is the other approach to maximize the therapeutic window by minimizing hyperphosphatemia. It has been hypothesized that FGFR1, 2 or 3, but not FGFR4, have a main role to regulate the phosphate and vitamin D homeostasis. In fact, hyperphosphatemia was not observed with fisogatinib, FGFR4 selective inhibitor, treatment at the dose that patients showed clinical responses in phase I trial. Although other FGFR4-inhibition driven on-target adverse effects have been confirmed, including nausea, vomiting, and diarrhea as dose limiting toxicity, the authors considered that these events were manageable with antiemetics and supportive care (Kim et al., 2019).

While the present findings in this research provide the potential of FGFR inhibitor to the unmet need of current therapies for cancers, further studies on these aspects as mentioned above will allow a broader characterization of the therapeutic potential of FGFR inhibitors. I hope that this research and future studies open the way of cancer patients.

Conclusion

As summary of this dissertation, important findings in current investigation are; I) Identification of ASP5878 as a novel, potent and selective FGFR inhibitors, II) Demonstration of ASP5878's dramatic anti-tumor efficacy for FGF19-expressing HCC, III) Identification of novel FGFR4 oncogenic mutation, G636C, in gastric cancer and IV) Demonstration of ASP5878's dramatic anti-tumor efficacy for G636C-FGFR4 positive tumor. Taken together, these findings show that ASP5878 may be promising candidates for cancer patients who have aberrant FGF19-FGFR4 signal such as FGF19-expression and G636C mutation.

I am confident that my research contributes to developing FGFR inhibitors for cancer patients with aberrant FGF19-FGFR4 signal and advancing our understanding of the disease mechanism. I strongly hope that my research will lead to the development of new drugs that will dramatically improve the oncology society.

Acknowledgements

I am deeply grateful to Professor Hiroyuki Ito, University of Tsukuba, for his continuous guidance and valuable discussions throughout my doctoral program. Also, I would like to express my gratitude to Professor Renu Wadhwa KAUL, Professor Makoto Miyagishi, Associate Professor Myra O Villareal and Associate Professor Yusaku Miyamae (University of Tsukuba) for their appropriate advice during the preparation of this dissertation.

Further, Mr. Hidetsugu Okada, Ms. Rumi Kihara, Dr. Tatsuya Kawase, Ms. Ayako Nakayama, Dr. Tomoyuki Suzuki, Dr. Minoru Kameda, Dr. Nobuaki Shindoh, Dr. Tadashi Terasaka, Dr. Masaaki Hirano and Dr. Sadao Kuromitsu gave insightful comments and suggestions for conducting and summarizing this research.

In chapter II, I thank Hiroshi Fushiki, Aya Kikuchi, Taisuke Nakazawa, Masateru Iizuka, and Hideki Sakagami for their involvement in this study.

References

- Cancer Genome Atlas Research Network. 2014, Comprehensive molecular characterization of urothelial bladder carcinoma. Nature 507, 315-322.
- Arao, T., Ueshima, K., Matsumoto, K., Nagai, T., Kimura, H., Hagiwara, S., Sakurai, T., Haji, S., Kanazawa, A., Hidaka, H., Iso, Y., Kubota, K., Shimada, M., Utsunomiya, T., Hirooka, M., Hiasa, Y., Toyoki, Y., Hakamada, K., Yasui, K., Kumada, T., Toyoda, H., Sato, S., Hisai, H., Kuzuya, T., Tsuchiya, K., Izumi, N., Arii, S., Nishio, K., Kudo, M., 2013. FGF3/FGF4 amplification and multiple lung metastases in responders to sorafenib in hepatocellular carcinoma. Hepatology 57, 1407-1415.
- Arkenau H, S.M., Hollebecque A, Mathewson A, Lemech C, Landers D, Frewer P, et al., 2014. A phase 1 expansion cohort of the fibroblast growth factor receptor (FGFR) inhibitor AZD4547 in patients (pts) with advanced gastric (GC) and gastroesophageal (GOJ) cancer. J. Clin. Oncol. 32:5s, 2014 (suppl; abstr 2620).
- Asaumi M, F.T., Hisamichi H, Iikubo K, Iwai Y, Kameda M, Kawamoto Y, Kuriwaki I, Miyasaka K, Moritomo H, Noda A, Okada H, Suzuki A, Suzuki T, Tokuzaki K, Tomiyama H, Tsunoyama K, 2013. Nitrogen-containing Aromatic Heterocyclic Compound, in: Astellas Pharma Inc., K.P.C., Ltd (Ed.). Astellas Pharma Inc., Kotobuki Pharm Co., Ltd.
- Bae, J.H., Lew, E.D., Yuzawa, S., Tome, F., Lax, I., Schlessinger, J., 2009. The selectivity of receptor tyrosine kinase signaling is controlled by a secondary SH2 domain binding site. Cell 138, 514-524.
- Bahleda R, D.R., Adamo B, Gazzah A, Jeffrey R, Bob Zhong, Suso J, et al, 2014. Phase 1 study of JNJ-42756493, a pan-fibroblast growth factor receptor (FGFR) inhibitor, in patients with advanced solid tumors. J. Clin. Oncol. 32:5s, (suppl; abstr 2501).
- Bang, Y.J., Van Cutsem, E., Feyereislova, A., Chung, H.C., Shen, L., Sawaki, A., Lordick, F., Ohtsu, A., Omuro, Y., Satoh, T., Aprile, G., Kulikov, E., Hill, J., Lehle, M., Ruschoff, J., Kang, Y.K., 2010. Trastuzumab in combination with chemotherapy versus chemotherapy alone for treatment of HER2-positive advanced gastric or gastro-oesophageal junction cancer (ToGA): a phase 3, open-label, randomised controlled trial. Lancet 376, 687-697.
- Beenken, A., Mohammadi, M., 2009. The FGF family: biology, pathophysiology and therapy. Nat Rev Drug Discov 8, 235-253.
- Belov, A.A., Mohammadi, M., 2013. Molecular mechanisms of fibroblast growth factor signaling in physiology and pathology. Cold Spring Harb Perspect Biol 5.
- Blundell, T.L., Sibanda, B.L., Sternberg, M.J., Thornton, J.M., 1987. Knowledge-based prediction of protein structures and the design of novel molecules. Nature 326, 347-352.
- Bray, F., Ferlay, J., Soerjomataram, I., Siegel, R.L., Torre, L.A., Jemal, A., 2018. Global cancer statistics 2018: GLOBOCAN estimates of incidence and mortality worldwide for 36 cancers in 185 countries. CA Cancer J Clin 68, 394-424.
- Brown, A.P., Courtney, C.L., King, L.M., Groom, S.C., Graziano, M.J., 2005. Cartilage dysplasia and tissue mineralization in the rat following administration of a FGF receptor tyrosine kinase inhibitor. Toxicol Pathol 33, 449-455.
- Campbell, J.D., Alexandrov, A., Kim, J., Wala, J., Berger, A.H., Pedamallu, C.S., Shukla, S.A., Guo, G., Brooks, A.N., Murray, B.A., Imielinski, M., Hu, X., Ling, S., Akbani, R., Rosenberg, M., Cibulskis, C., Ramachandran, A., Collisson, E.A., Kwiatkowski, D.J., Lawrence, M.S., Weinstein, J.N., Verhaak, R.G., Wu, C.J., Hammerman,

P.S., Cherniack, A.D., Getz, G., Artyomov, M.N., Schreiber, R., Govindan, R., Meyerson, M., 2016. Distinct patterns of somatic genome alterations in lung adenocarcinomas and squamous cell carcinomas. Nat Genet 48, 607-616.

- Chen, H., Ma, J., Li, W., Eliseenkova, A.V., Xu, C., Neubert, T.A., Miller, W.T., Mohammadi, M., 2007. A molecular brake in the kinase hinge region regulates the activity of receptor tyrosine kinases. Mol Cell 27, 717-730.
- Chen, H., Marsiglia, W.M., Cho, M.K., Huang, Z., Deng, J., Blais, S.P., Gai, W., Bhattacharya, S., Neubert, T.A., Traaseth, N.J., Mohammadi, M., 2017. Elucidation of a four-site allosteric network in fibroblast growth factor receptor tyrosine kinases. Elife 6.
- Chen, H., Xu, C.F., Ma, J., Eliseenkova, A.V., Li, W., Pollock, P.M., Pitteloud, N., Miller, W.T., Neubert, T.A., Mohammadi, M., 2008. A crystallographic snapshot of tyrosine trans-phosphorylation in action. Proc Natl Acad Sci U S A 105, 19660-19665.
- Cheng, A.L., Kang, Y.K., Chen, Z., Tsao, C.J., Qin, S., Kim, J.S., Luo, R., Feng, J., Ye, S., Yang, T.S., Xu, J., Sun, Y., Liang, H., Liu, J., Wang, J., Tak, W.Y., Pan, H., Burock, K., Zou, J., Voliotis, D., Guan, Z., 2009. Efficacy and safety of sorafenib in patients in the Asia-Pacific region with advanced hepatocellular carcinoma: a phase III randomised, double-blind, placebo-controlled trial. Lancet Oncol 10, 25-34.
- Chong, I.Y., Cunningham, D., Barber, L.J., Campbell, J., Chen, L., Kozarewa, I., Fenwick, K., Assiotis, I., Guettler, S., Garcia-Murillas, I., Awan, S., Lambros, M., Starling, N., Wotherspoon, A., Stamp, G., Gonzalez-de-Castro, D., Benson, M., Chau, I., Hulkki, S., Nohadani, M., Eltahir, Z., Lemnrau, A., Orr, N., Rao, S., Lord, C.J., Ashworth, A., 2013. The genomic landscape of oesophagogastric junctional adenocarcinoma. J Pathol 231, 301-310.
- Cocco, E., Scaltriti, M., Drilon, A., 2018. NTRK fusion-positive cancers and TRK inhibitor therapy. Nat Rev Clin Oncol 15, 731-747.
- Desnoyers, L.R., Pai, R., Ferrando, R.E., Hotzel, K., Le, T., Ross, J., Carano, R., D'Souza, A., Qing, J., Mohtashemi, I., Ashkenazi, A., French, D.M., 2008. Targeting FGF19 inhibits tumor growth in colon cancer xenograft and FGF19 transgenic hepatocellular carcinoma models. Oncogene 27, 85-97.
- Dienstmann, R., Brana, I., Rodon, J., Tabernero, J., 2011. Toxicity as a biomarker of efficacy of molecular targeted therapies: focus on EGFR and VEGF inhibiting anticancer drugs. Oncologist 16, 1729-1740.
- Doi, I., 1976. Establishment of a cell line and its clonal sublines from a patient with hepatoblastoma. Gan 67, 1-10.
- Dor, I., Namba, M., Sato, J., 1975. Establishment and some biological characteristics of human hepatoma cell lines. Gan 66, 385-392.
- French, D.M., Lin, B.C., Wang, M., Adams, C., Shek, T., Hotzel, K., Bolon, B., Ferrando, R., Blackmore, C., Schroeder, K., Rodriguez, L.A., Hristopoulos, M., Venook, R., Ashkenazi, A., Desnoyers, L.R., 2012. Targeting FGFR4 inhibits hepatocellular carcinoma in preclinical mouse models. PLoS One 7, e36713.
- Fu, L., John, L.M., Adams, S.H., Yu, X.X., Tomlinson, E., Renz, M., Williams, P.M., Soriano, R., Corpuz, R., Moffat, B., Vandlen, R., Simmons, L., Foster, J., Stephan, J.P., Tsai, S.P., Stewart, T.A., 2004. Fibroblast growth factor 19 increases metabolic rate and reverses dietary and leptin-deficient diabetes. Endocrinology 145, 2594-2603.
- Futami, T., Okada, H., Kihara, R., Kawase, T., Nakayama, A., Suzuki, T., Kameda, M., Shindoh, N., Terasaka, T., Hirano, M., Kuromitsu, S., 2017. ASP5878, a Novel Inhibitor of FGFR1, 2, 3, and 4, Inhibits the Growth of

FGF19-Expressing Hepatocellular Carcinoma. Mol Cancer Ther 16, 68-75.

- Gallo, L.H., Nelson, K.N., Meyer, A.N., Donoghue, D.J., 2015. Functions of Fibroblast Growth Factor Receptors in cancer defined by novel translocations and mutations. Cytokine Growth Factor Rev 26, 425-449.
- Gao, Q., Liang, W.W., Foltz, S.M., Mutharasu, G., Jayasinghe, R.G., Cao, S., Liao, W.W., Reynolds, S.M., Wyczalkowski, M.A., Yao, L., Yu, L., Sun, S.Q., Chen, K., Lazar, A.J., Fields, R.C., Wendl, M.C., Van Tine, B.A., Vij, R., Chen, F., Nykter, M., Shmulevich, I., Ding, L., 2018. Driver Fusions and Their Implications in the Development and Treatment of Human Cancers. Cell Rep 23, 227-238.e223.
- Gavine, P.R., Mooney, L., Kilgour, E., Thomas, A.P., Al-Kadhimi, K., Beck, S., Rooney, C., Coleman, T., Baker, D., Mellor, M.J., Brooks, A.N., Klinowska, T., 2012. AZD4547: an orally bioavailable, potent, and selective inhibitor of the fibroblast growth factor receptor tyrosine kinase family. Cancer Res 72, 2045-2056.
- Gu, Q., Zhang, B., Sun, H., Xu, Q., Tan, Y., Wang, G., Luo, Q., Xu, W., Yang, S., Li, J., Fu, J., Chen, L., Yuan, S., Liang, G., Ji, Q., Chen, S.H., Chan, C.C., Zhou, W., Xu, X., Wang, H., Fang, D.D., 2015. Genomic characterization of a large panel of patient-derived hepatocellular carcinoma xenograft tumor models for preclinical development. Oncotarget 6, 20160-20176.
- Guagnano, V., Furet, P., Spanka, C., Bordas, V., Le Douget, M., Stamm, C., Brueggen, J., Jensen, M.R., Schnell, C., Schmid, H., Wartmann, M., Berghausen, J., Drueckes, P., Zimmerlin, A., Bussiere, D., Murray, J., Graus Porta, D., 2011. Discovery of 3-(2,6-dichloro-3,5-dimethoxy-phenyl)-1-{6-[4-(4-ethyl-piperazin-1-yl)-phenylamin o]-pyrimidin-4-yl}-1-methyl-urea (NVP-BGJ398), a potent and selective inhibitor of the fibroblast growth factor receptor family of receptor tyrosine kinase. J Med Chem 54, 7066-7083.
- Guagnano, V., Kauffmann, A., Wohrle, S., Stamm, C., Ito, M., Barys, L., Pornon, A., Yao, Y., Li, F., Zhang, Y., Chen, Z., Wilson, C.J., Bordas, V., Le Douget, M., Gaither, L.A., Borawski, J., Monahan, J.E., Venkatesan, K., Brummendorf, T., Thomas, D.M., Garcia-Echeverria, C., Hofmann, F., Sellers, W.R., Graus-Porta, D., 2012. FGFR genetic alterations predict for sensitivity to NVP-BGJ398, a selective pan-FGFR inhibitor. Cancer Discov 2, 1118-1133.
- Gunasekaran, K., Ramakrishnan, C., Balaram, P., 1997. Beta-hairpins in proteins revisited: lessons for de novo design. Protein Eng 10, 1131-1141.
- Hagel, M., Miduturu, C., Sheets, M., Rubin, N., Weng, W., Stransky, N., Bifulco, N., Kim, J.L., Hodous, B., Brooijmans, N., Shutes, A., Winter, C., Lengauer, C., Kohl, N.E., Guzi, T., 2015. First Selective Small Molecule Inhibitor of FGFR4 for the Treatment of Hepatocellular Carcinomas with an Activated FGFR4 Signaling Pathway. Cancer Discov 5, 424-437.
- Harimoto, N., Taguchi, K., Shirabe, K., Adachi, E., Sakaguchi, Y., Toh, Y., Okamura, T., Kayashima, H., Taketomi, A., Maehara, Y., 2010. The significance of fibroblast growth factor receptor 2 expression in differentiation of hepatocellular carcinoma. Oncology 78, 361-368.
- Helsten, T., Elkin, S., Arthur, E., Tomson, B.N., Carter, J., Kurzrock, R., 2016. The FGFR Landscape in Cancer: Analysis of 4,853 Tumors by Next-Generation Sequencing. Clin Cancer Res 22, 259-267.
- Hierro, C., Alsina, M., Sanchez, M., Serra, V., Rodon, J., Tabernero, J., 2017. Targeting the fibroblast growth factor receptor 2 in gastric cancer: promise or pitfall? Ann Oncol 28, 1207-1216.
- Hierro, C., Rodon, J., Tabernero, J., 2015. Fibroblast Growth Factor (FGF) Receptor/FGF Inhibitors: Novel Targets and Strategies for Optimization of Response of Solid Tumors. Semin Oncol 42, 801-819.
- Homma, S., 1985. Studies on the establishment and some biological characteristics of cultured human liver cancer

cell lines; thir growth, functional and morphological characteristics and temperature sensitivities. Jikeikai Med. J. 32, 289-315.

- Hudis, C.A., 2007. Trastuzumab--mechanism of action and use in clinical practice. N Engl J Med 357, 39-51.
- Huh, N., Utakoji, T., 1981. Production of HBs-antigen by two new human hepatoma cell lines and its enhancement by dexamethasone. Gan 72, 178-179.
- Hyeon, J., Ahn, S., Lee, J.J., Song, D.H., Park, C.K., 2013. Expression of fibroblast growth factor 19 is associated with recurrence and poor prognosis of hepatocellular carcinoma. Dig Dis Sci 58, 1916-1922.
- Jeske, Y.W., Ali, S., Byron, S.A., Gao, F., Mannel, R.S., Ghebre, R.G., DiSilvestro, P.A., Lele, S.B., Pearl, M.L., Schmidt, A.P., Lankes, H.A., Ramirez, N.C., Rasty, G., Powell, M., Goodfellow, P.J., Pollock, P.M., 2017. FGFR2 mutations are associated with poor outcomes in endometrioid endometrial cancer: An NRG Oncology/Gynecologic Oncology Group study. Gynecol Oncol 145, 366-373.
- Johnson, D.E., Lu, J., Chen, H., Werner, S., Williams, L.T., 1991. The human fibroblast growth factor receptor genes: a common structural arrangement underlies the mechanisms for generating receptor forms that differ in their third immunoglobulin domain. Mol Cell Biol 11, 4627-4634.
- Kakiuchi, M., Nishizawa, T., Ueda, H., Gotoh, K., Tanaka, A., Hayashi, A., Yamamoto, S., Tatsuno, K., Katoh, H., Watanabe, Y., Ichimura, T., Ushiku, T., Funahashi, S., Tateishi, K., Wada, I., Shimizu, N., Nomura, S., Koike, K., Seto, Y., Fukayama, M., Aburatani, H., Ishikawa, S., 2014. Recurrent gain-of-function mutations of RHOA in diffuse-type gastric carcinoma. Nat Genet 46, 583-587.
- Katoh, M., 2019. Fibroblast growth factor receptors as treatment targets in clinical oncology. Nat Rev Clin Oncol 16, 105-122.
- Kharitonenkov, A., Shiyanova, T.L., Koester, A., Ford, A.M., Micanovic, R., Galbreath, E.J., Sandusky, G.E., Hammond, L.J., Moyers, J.S., Owens, R.A., Gromada, J., Brozinick, J.T., Hawkins, E.D., Wroblewski, V.J., Li, D.S., Mehrbod, F., Jaskunas, S.R., Shanafelt, A.B., 2005. FGF-21 as a novel metabolic regulator. J Clin Invest 115, 1627-1635.
- Kikuchi, A., Suzuki, T., Nakazawa, T., Iizuka, M., Nakayama, A., Ozawa, T., Kameda, M., Shindoh, N., Terasaka, T., Hirano, M., Kuromitsu, S., 2017. ASP5878, a selective FGFR inhibitor, to treat FGFR3-dependent urothelial cancer with or without chemoresistance. Cancer Sci 108, 236-242.
- Kim, R.D., Sarker, D., Meyer, T., Yau, T., Macarulla, T., Park, J.W., Choo, S.P., Hollebecque, A., Sung, M.W., Lim, H.Y., Mazzaferro, V., Trojan, J., Zhu, A.X., Yoon, J.H., Sharma, S., Lin, Z.Z., Chan, S.L., Faivre, S., Feun, L.G., Yen, C.J., Dufour, J.F., Palmer, D.H., Llovet, J.M., Manoogian, M., Tugnait, M., Stransky, N., Hagel, M., Kohl, N.E., Lengauer, C., Sherwin, C.A., Schmidt-Kittler, O., Hoeflich, K.P., Shi, H., Wolf, B.B., Kang, Y.K., 2019. First-in-Human Phase I Study of Fisogatinib (BLU-554) Validates Aberrant FGF19 Signaling as a Driver Event in Hepatocellular Carcinoma. Cancer Discov 9, 1696-1707.
- Kong, K., Ng, P.K., Scott, K.L., 2017. Ba/F3 transformation assays, Oncotarget, United States, pp. 35488-35489.
- Lang, L., Shull, A.Y., Teng, Y., 2019. Interrupting the FGF19-FGFR4 Axis to Therapeutically Disrupt Cancer Progression. Curr Cancer Drug Targets 19, 17-25.
- Lee, Y.T., Tan, Y.J., Oon, C.E., 2018. Molecular targeted therapy: Treating cancer with specificity. Eur J Pharmacol 834, 188-196.
- Lesca, E., Lammens, A., Huber, R., Augustin, M., 2014. Structural analysis of the human fibroblast growth factor receptor 4 kinase. J Mol Biol 426, 3744-3756.

- Liang, G., Chen, G., Wei, X., Zhao, Y., Li, X., 2013. Small molecule inhibition of fibroblast growth factor receptors in cancer. Cytokine Growth Factor Rev 24, 467-475.
- Lin, B.C., Desnoyers, L.R., 2012. FGF19 and cancer. Adv Exp Med Biol 728, 183-194.
- Liu, X., Meltzer, S.J., 2017. Gastric Cancer in the Era of Precision Medicine. Cell Mol Gastroenterol Hepatol 3, 348-358.
- Lott, S., Wang, M., Zhang, S., MacLennan, G.T., Lopez-Beltran, A., Montironi, R., Sung, M.T., Tan, P.H., Cheng, L., 2009. FGFR3 and TP53 mutation analysis in inverted urothelial papilloma: incidence and etiological considerations. Mod Pathol 22, 627-632.
- Luo, J., Liu, S., Leung, S., Gru, A.A., Tao, Y., Hoog, J., Ho, J., Davies, S.R., Allred, D.C., Salavaggione, A.L., Snider, J., Mardis, E.R., Nielsen, T.O., Ellis, M.J., 2017. An mRNA Gene Expression-Based Signature to Identify FGFR1-Amplified Estrogen Receptor-Positive Breast Tumors. J Mol Diagn 19, 147-161.
- Malik, S.M., Maher, V.E., Bijwaard, K.E., Becker, R.L., Zhang, L., Tang, S.W., Song, P., Liu, Q., Marathe, A., Gehrke, B., Helms, W., Hanner, D., Justice, R., Pazdur, R., 2014. U.S. Food and Drug Administration approval: crizotinib for treatment of advanced or metastatic non-small cell lung cancer that is anaplastic lymphoma kinase positive. Clin Cancer Res 20, 2029-2034.
- Mariotto, A.B., Yabroff, K.R., Shao, Y., Feuer, E.J., Brown, M.L., 2011. Projections of the cost of cancer care in the United States: 2010-2020. J Natl Cancer Inst 103, 117-128.
- Milner-White, E.J., Poet, R., 1986. Four classes of beta-hairpins in proteins. Biochem J 240, 289-292.
- Miura, S., Mitsuhashi, N., Shimizu, H., Kimura, F., Yoshidome, H., Otsuka, M., Kato, A., Shida, T., Okamura, D., Miyazaki, M., 2012. Fibroblast growth factor 19 expression correlates with tumor progression and poorer prognosis of hepatocellular carcinoma. BMC Cancer 12, 56.
- Morimoto, Y., Ozaki, T., Ouchida, M., Umehara, N., Ohata, N., Yoshida, A., Shimizu, K., Inoue, H., 2003. Single nucleotide polymorphism in fibroblast growth factor receptor 4 at codon 388 is associated with prognosis in high-grade soft tissue sarcoma. Cancer 98, 2245-2250.
- Murray, C.J., Vos, T., Lozano, R., Naghavi, M., Flaxman, A.D., Michaud, C., Ezzati, M., Shibuya, K., Salomon, J.A., Abdalla, S., Aboyans, V., Abraham, J., Ackerman, I., Aggarwal, R., Ahn, S.Y., Ali, M.K., Alvarado, M., Anderson, H.R., Anderson, L.M., Andrews, K.G., Atkinson, C., Baddour, L.M., Bahalim, A.N., Barker-Collo, S., Barrero, L.H., Bartels, D.H., Basanez, M.G., Baxter, A., Bell, M.L., Benjamin, E.J., Bennett, D., Bernabe, E., Bhalla, K., Bhandari, B., Bikbov, B., Bin Abdulhak, A., Birbeck, G., Black, J.A., Blencowe, H., Blore, J.D., Blyth, F., Bolliger, I., Bonaventure, A., Boufous, S., Bourne, R., Boussinesq, M., Braithwaite, T., Brayne, C., Bridgett, L., Brooker, S., Brooks, P., Brugha, T.S., Bryan-Hancock, C., Bucello, C., Buchbinder, R., Buckle, G., Budke, C.M., Burch, M., Burney, P., Burstein, R., Calabria, B., Campbell, B., Canter, C.E., Carabin, H., Carapetis, J., Carmona, L., Cella, C., Charlson, F., Chen, H., Cheng, A.T., Chou, D., Chugh, S.S., Coffeng, L.E., Colan, S.D., Colquhoun, S., Colson, K.E., Condon, J., Connor, M.D., Cooper, L.T., Corriere, M., Cortinovis, M., de Vaccaro, K.C., Couser, W., Cowie, B.C., Criqui, M.H., Cross, M., Dabhadkar, K.C., Dahiya, M., Dahodwala, N., Damsere-Derry, J., Danaei, G., Davis, A., De Leo, D., Degenhardt, L., Dellavalle, R., Delossantos, A., Denenberg, J., Derrett, S., Des Jarlais, D.C., Dharmaratne, S.D., Dherani, M., Diaz-Torne, C., Dolk, H., Dorsey, E.R., Driscoll, T., Duber, H., Ebel, B., Edmond, K., Elbaz, A., Ali, S.E., Erskine, H., Erwin, P.J., Espindola, P., Ewoigbokhan, S.E., Farzadfar, F., Feigin, V., Felson, D.T., Ferrari, A., Ferri, C.P., Fevre, E.M., Finucane, M.M., Flaxman, S., Flood, L., Foreman, K., Forouzanfar, M.H., Fowkes, F.G., Fransen, M., Freeman, M.K., Gabbe, B.J., Gabriel,

S.E., Gakidou, E., Ganatra, H.A., Garcia, B., Gaspari, F., Gillum, R.F., Gmel, G., Gonzalez-Medina, D., Gosselin, R., Grainger, R., Grant, B., Groeger, J., Guillemin, F., Gunnell, D., Gupta, R., Haagsma, J., Hagan, H., Halasa, Y.A., Hall, W., Haring, D., Haro, J.M., Harrison, J.E., Havmoeller, R., Hay, R.J., Higashi, H., Hill, C., Hoen, B., Hoffman, H., Hotez, P.J., Hoy, D., Huang, J.J., Ibeanusi, S.E., Jacobsen, K.H., James, S.L., Jarvis, D., Jasrasaria, R., Jayaraman, S., Johns, N., Jonas, J.B., Karthikeyan, G., Kassebaum, N., Kawakami, N., Keren, A., Khoo, J.P., King, C.H., Knowlton, L.M., Kobusingye, O., Koranteng, A., Krishnamurthi, R., Laden, F., Lalloo, R., Laslett, L.L., Lathlean, T., Leasher, J.L., Lee, Y.Y., Leigh, J., Levinson, D., Lim, S.S., Limb, E., Lin, J.K., Lipnick, M., Lipshultz, S.E., Liu, W., Loane, M., Ohno, S.L., Lyons, R., Mabweijano, J., MacIntyre, M.F., Malekzadeh, R., Mallinger, L., Manivannan, S., Marcenes, W., March, L., Margolis, D.J., Marks, G.B., Marks, R., Matsumori, A., Matzopoulos, R., Mayosi, B.M., McAnulty, J.H., McDermott, M.M., McGill, N., McGrath, J., Medina-Mora, M.E., Meltzer, M., Mensah, G.A., Merriman, T.R., Meyer, A.C., Miglioli, V., Miller, M., Miller, T.R., Mitchell, P.B., Mock, C., Mocumbi, A.O., Moffitt, T.E., Mokdad, A.A., Monasta, L., Montico, M., Moradi-Lakeh, M., Moran, A., Morawska, L., Mori, R., Murdoch, M.E., Mwaniki, M.K., Naidoo, K., Nair, M.N., Naldi, L., Narayan, K.M., Nelson, P.K., Nelson, R.G., Nevitt, M.C., Newton, C.R., Nolte, S., Norman, P., Norman, R., O'Donnell, M., O'Hanlon, S., Olives, C., Omer, S.B., Ortblad, K., Osborne, R., Ozgediz, D., Page, A., Pahari, B., Pandian, J.D., Rivero, A.P., Patten, S.B., Pearce, N., Padilla, R.P., Perez-Ruiz, F., Perico, N., Pesudovs, K., Phillips, D., Phillips, M.R., Pierce, K., Pion, S., Polanczyk, G.V., Polinder, S., Pope, C.A., 3rd, Popova, S., Porrini, E., Pourmalek, F., Prince, M., Pullan, R.L., Ramaiah, K.D., Ranganathan, D., Razavi, H., Regan, M., Rehm, J.T., Rein, D.B., Remuzzi, G., Richardson, K., Rivara, F.P., Roberts, T., Robinson, C., De Leon, F.R., Ronfani, L., Room, R., Rosenfeld, L.C., Rushton, L., Sacco, R.L., Saha, S., Sampson, U., Sanchez-Riera, L., Sanman, E., Schwebel, D.C., Scott, J.G., Segui-Gomez, M., Shahraz, S., Shepard, D.S., Shin, H., Shivakoti, R., Singh, D., Singh, G.M., Singh, J.A., Singleton, J., Sleet, D.A., Sliwa, K., Smith, E., Smith, J.L., Stapelberg, N.J., Steer, A., Steiner, T., Stolk, W.A., Stovner, L.J., Sudfeld, C., Syed, S., Tamburlini, G., Tavakkoli, M., Taylor, H.R., Taylor, J.A., Taylor, W.J., Thomas, B., Thomson, W.M., Thurston, G.D., Tleyjeh, I.M., Tonelli, M., Towbin, J.A., Truelsen, T., Tsilimbaris, M.K., Ubeda, C., Undurraga, E.A., van der Werf, M.J., van Os, J., Vavilala, M.S., Venketasubramanian, N., Wang, M., Wang, W., Watt, K., Weatherall, D.J., Weinstock, M.A., Weintraub, R., Weisskopf, M.G., Weissman, M.M., White, R.A., Whiteford, H., Wiebe, N., Wiersma, S.T., Wilkinson, J.D., Williams, H.C., Williams, S.R., Witt, E., Wolfe, F., Woolf, A.D., Wulf, S., Yeh, P.H., Zaidi, A.K., Zheng, Z.J., Zonies, D., Lopez, A.D., AlMazroa, M.A., Memish, Z.A., 2012. Disability-adjusted life years (DALYs) for 291 diseases and injuries in 21 regions, 1990-2010: a systematic analysis for the Global Burden of Disease Study 2010. Lancet 380, 2197-2223.

- Nakabayashi, H., Taketa, K., Miyano, K., Yamane, T., Sato, J., 1982. Growth of human hepatoma cells lines with differentiated functions in chemically defined medium. Cancer Res 42, 3858-3863.
- Nicholes, K., Guillet, S., Tomlinson, E., Hillan, K., Wright, B., Frantz, G.D., Pham, T.A., Dillard-Telm, L., Tsai, S.P., Stephan, J.P., Stinson, J., Stewart, T., French, D.M., 2002. A mouse model of hepatocellular carcinoma: ectopic expression of fibroblast growth factor 19 in skeletal muscle of transgenic mice. Am J Pathol 160, 2295-2307.
- Nyeng, P., Norgaard, G.A., Kobberup, S., Jensen, J., 2007. FGF10 signaling controls stomach morphogenesis. Dev Biol 303, 295-310.
- Ornitz, D.M., Itoh, N., 2015. The Fibroblast Growth Factor signaling pathway. Wiley Interdiscip Rev Dev Biol 4, 215-266.

- Pao, W., Miller, V., Zakowski, M., Doherty, J., Politi, K., Sarkaria, I., Singh, B., Heelan, R., Rusch, V., Fulton, L., Mardis, E., Kupfer, D., Wilson, R., Kris, M., Varmus, H., 2004. EGF receptor gene mutations are common in lung cancers from "never smokers" and are associated with sensitivity of tumors to gefitinib and erlotinib. Proc Natl Acad Sci U S A 101, 13306-13311.
- Park, J.G., Lee, J.H., Kang, M.S., Park, K.J., Jeon, Y.M., Lee, H.J., Kwon, H.S., Park, H.S., Yeo, K.S., Lee, K.U., et al., 1995. Characterization of cell lines established from human hepatocellular carcinoma. Int J Cancer 62, 276-282.
- Patani, H., Bunney, T.D., Thiyagarajan, N., Norman, R.A., Ogg, D., Breed, J., Ashford, P., Potterton, A., Edwards, M., Williams, S.V., Thomson, G.S., Pang, C.S., Knowles, M.A., Breeze, A.L., Orengo, C., Phillips, C., Katan, M., 2016. Landscape of activating cancer mutations in FGFR kinases and their differential responses to inhibitors in clinical use. Oncotarget 7, 24252-24268.
- Paur, J., Nika, L., Maier, C., Moscu-Gregor, A., Kostka, J., Huber, D., Mohr, T., Heffeter, P., Schrottmaier, W.C., Kappel, S., Kandioler, D., Holzmann, K., Marian, B., Berger, W., Grusch, M., Grasl-Kraupp, B., 2015. Fibroblast growth factor receptor 3 isoforms: Novel therapeutic targets for hepatocellular carcinoma? Hepatology 62, 1767-1778.
- Peifer, M., Fernandez-Cuesta, L., Sos, M.L., George, J., Seidel, D., Kasper, L.H., Plenker, D., Leenders, F., Sun, R., Zander, T., Menon, R., Koker, M., Dahmen, I., Muller, C., Di Cerbo, V., Schildhaus, H.U., Altmuller, J., Baessmann, I., Becker, C., de Wilde, B., Vandesompele, J., Bohm, D., Ansen, S., Gabler, F., Wilkening, I., Heynck, S., Heuckmann, J.M., Lu, X., Carter, S.L., Cibulskis, K., Banerji, S., Getz, G., Park, K.S., Rauh, D., Grutter, C., Fischer, M., Pasqualucci, L., Wright, G., Wainer, Z., Russell, P., Petersen, I., Chen, Y., Stoelben, E., Ludwig, C., Schnabel, P., Hoffmann, H., Muley, T., Brockmann, M., Engel-Riedel, W., Muscarella, L.A., Fazio, V.M., Groen, H., Timens, W., Sietsma, H., Thunnissen, E., Smit, E., Heideman, D.A., Snijders, P.J., Cappuzzo, F., Ligorio, C., Damiani, S., Field, J., Solberg, S., Brustugun, O.T., Lund-Iversen, M., Sanger, J., Clement, J.H., Soltermann, A., Moch, H., Weder, W., Solomon, B., Soria, J.C., Validire, P., Besse, B., Brambilla, E., Brambilla, C., Lantuejoul, S., Lorimier, P., Schneider, P.M., Hallek, M., Pao, W., Meyerson, M., Sage, J., Shendure, J., Schneider, R., Buttner, R., Wolf, J., Nurnberg, P., Perner, S., Heukamp, L.C., Brindle, P.K., Haas, S., Thomas, R.K., 2012. Integrative genome analyses identify key somatic driver mutations of small-cell lung cancer. Nat Genet 44, 1104-1110.
- Perera, T.P.S., Jovcheva, E., Mevellec, L., Vialard, J., De Lange, D., Verhulst, T., Paulussen, C., Van De Ven, K., King, P., Freyne, E., Rees, D.C., Squires, M., Saxty, G., Page, M., Murray, C.W., Gilissen, R., Ward, G., Thompson, N.T., Newell, D.R., Cheng, N., Xie, L., Yang, J., Platero, S.J., Karkera, J.D., Moy, C., Angibaud, P., Laquerre, S., Lorenzi, M.V., 2017. Discovery and Pharmacological Characterization of JNJ-42756493 (Erdafitinib), a Functionally Selective Small-Molecule FGFR Family Inhibitor. Mol Cancer Ther 16, 1010-1020.
- Poon, R.T., 2011. Prevention of recurrence after resection of hepatocellular carcinoma: a daunting challenge. Hepatology 54, 757-759.
- Qiu, W.H., Zhou, B.S., Chu, P.G., Chen, W.G., Chung, C., Shih, J., Hwu, P., Yeh, C., Lopez, R., Yen, Y., 2005. Over-expression of fibroblast growth factor receptor 3 in human hepatocellular carcinoma. World J Gastroenterol 11, 5266-5272.
- Razzaque, M.S., Lanske, B., 2007. The emerging role of the fibroblast growth factor-23-klotho axis in renal regulation of phosphate homeostasis. J Endocrinol 194, 1-10.

- Roidl, A., Foo, P., Wong, W., Mann, C., Bechtold, S., Berger, H.J., Streit, S., Ruhe, J.E., Hart, S., Ullrich, A., Ho, H.K., 2010. The FGFR4 Y367C mutant is a dominant oncogene in MDA-MB453 breast cancer cells. Oncogene 29, 1543-1552.
- Romond, E.H., Perez, E.A., Bryant, J., Suman, V.J., Geyer, C.E., Jr., Davidson, N.E., Tan-Chiu, E., Martino, S., Paik, S., Kaufman, P.A., Swain, S.M., Pisansky, T.M., Fehrenbacher, L., Kutteh, L.A., Vogel, V.G., Visscher, D.W., Yothers, G., Jenkins, R.B., Brown, A.M., Dakhil, S.R., Mamounas, E.P., Lingle, W.L., Klein, P.M., Ingle, J.N., Wolmark, N., 2005. Trastuzumab plus adjuvant chemotherapy for operable HER2-positive breast cancer. N Engl J Med 353, 1673-1684.
- Sandhu, D.S., Baichoo, E., Roberts, L.R., 2014. Fibroblast growth factor signaling in liver carcinogenesis. Hepatology 59, 1166-1173.
- Sawey, E.T., Chanrion, M., Cai, C., Wu, G., Zhang, J., Zender, L., Zhao, A., Busuttil, R.W., Yee, H., Stein, L., French, D.M., Finn, R.S., Lowe, S.W., Powers, S., 2011. Identification of a therapeutic strategy targeting amplified FGF19 in liver cancer by Oncogenomic screening. Cancer Cell 19, 347-358.
- Spangenberg, H.C., Thimme, R., Blum, H.E., 2009. Targeted therapy for hepatocellular carcinoma. Nat Rev Gastroenterol Hepatol 6, 423-432.
- Strumberg, D., Richly, H., Hilger, R.A., Schleucher, N., Korfee, S., Tewes, M., Faghih, M., Brendel, E., Voliotis, D., Haase, C.G., Schwartz, B., Awada, A., Voigtmann, R., Scheulen, M.E., Seeber, S., 2005. Phase I clinical and pharmacokinetic study of the Novel Raf kinase and vascular endothelial growth factor receptor inhibitor BAY 43-9006 in patients with advanced refractory solid tumors. J Clin Oncol 23, 965-972.
- Tanner, Y., Grose, R.P., 2016. Dysregulated FGF signalling in neoplastic disorders. Semin Cell Dev Biol 53, 126-135.
- Taylor, J.G.t., Cheuk, A.T., Tsang, P.S., Chung, J.Y., Song, Y.K., Desai, K., Yu, Y., Chen, Q.R., Shah, K., Youngblood, V., Fang, J., Kim, S.Y., Yeung, C., Helman, L.J., Mendoza, A., Ngo, V., Staudt, L.M., Wei, J.S., Khanna, C., Catchpoole, D., Qualman, S.J., Hewitt, S.M., Merlino, G., Chanock, S.J., Khan, J., 2009. Identification of FGFR4-activating mutations in human rhabdomyosarcomas that promote metastasis in xenotransplanted models. J Clin Invest 119, 3395-3407.
- Tchaicha, J.H., Akbay, E.A., Altabef, A., Mikse, O.R., Kikuchi, E., Rhee, K., Liao, R.G., Bronson, R.T., Sholl, L.M., Meyerson, M., Hammerman, P.S., Wong, K.K., 2014. Kinase domain activation of FGFR2 yields high-grade lung adenocarcinoma sensitive to a Pan-FGFR inhibitor in a mouse model of NSCLC. Cancer Res 74, 4676-4684.
- Tomlinson, E., Fu, L., John, L., Hultgren, B., Huang, X., Renz, M., Stephan, J.P., Tsai, S.P., Powell-Braxton, L., French, D., Stewart, T.A., 2002. Transgenic mice expressing human fibroblast growth factor-19 display increased metabolic rate and decreased adiposity. Endocrinology 143, 1741-1747.
- Turner, N., Grose, R., 2010. Fibroblast growth factor signalling: from development to cancer. Nat Rev Cancer 10, 116-129.
- Turner, N., Lambros, M.B., Horlings, H.M., Pearson, A., Sharpe, R., Natrajan, R., Geyer, F.C., van Kouwenhove, M., Kreike, B., Mackay, A., Ashworth, A., van de Vijver, M.J., Reis-Filho, J.S., 2010. Integrative molecular profiling of triple negative breast cancers identifies amplicon drivers and potential therapeutic targets. Oncogene 29, 2013-2023.
- Verstraete, M., Debucquoy, A., Gonnissen, A., Dok, R., Isebaert, S., Devos, E., McBride, W., Haustermans, K.,

2015. In vitro and in vivo evaluation of the radiosensitizing effect of a selective FGFR inhibitor (JNJ-42756493) for rectal cancer. BMC Cancer 15, 946.

- Wang, J., Yu, W., Cai, Y., Ren, C., Ittmann, M.M., 2008. Altered fibroblast growth factor receptor 4 stability promotes prostate cancer progression. Neoplasia 10, 847-856.
- Weiss, J., Sos, M.L., Seidel, D., Peifer, M., Zander, T., Heuckmann, J.M., Ullrich, R.T., Menon, R., Maier, S., Soltermann, A., Moch, H., Wagener, P., Fischer, F., Heynck, S., Koker, M., Schottle, J., Leenders, F., Gabler, F., Dabow, I., Querings, S., Heukamp, L.C., Balke-Want, H., Ansen, S., Rauh, D., Baessmann, I., Altmuller, J., Wainer, Z., Conron, M., Wright, G., Russell, P., Solomon, B., Brambilla, E., Brambilla, C., Lorimier, P., Sollberg, S., Brustugun, O.T., Engel-Riedel, W., Ludwig, C., Petersen, I., Sanger, J., Clement, J., Groen, H., Timens, W., Sietsma, H., Thunnissen, E., Smit, E., Heideman, D., Cappuzzo, F., Ligorio, C., Damiani, S., Hallek, M., Beroukhim, R., Pao, W., Klebl, B., Baumann, M., Buettner, R., Ernestus, K., Stoelben, E., Wolf, J., Nurnberg, P., Perner, S., Thomas, R.K., 2010. Frequent and focal FGFR1 amplification associates with therapeutically tractable FGFR1 dependency in squamous cell lung cancer. Sci Transl Med 2, 62ra93.
- Wu, Y.M., Su, F., Kalyana-Sundaram, S., Khazanov, N., Ateeq, B., Cao, X., Lonigro, R.J., Vats, P., Wang, R., Lin, S.F., Cheng, A.J., Kunju, L.P., Siddiqui, J., Tomlins, S.A., Wyngaard, P., Sadis, S., Roychowdhury, S., Hussain, M.H., Feng, F.Y., Zalupski, M.M., Talpaz, M., Pienta, K.J., Rhodes, D.R., Robinson, D.R., Chinnaiyan, A.M., 2013. Identification of targetable FGFR gene fusions in diverse cancers. Cancer Discov 3, 636-647.
- Yamamoto, N., Ryoo, B.Y., Keam, B., Kudo, M., Lin, C.C., Kunieda, F., Ball, H.A., Moran, D., Komatsu, K., Takeda, K., Fukuda, M., Furuse, J., Morita, S., Doi, T., 2019. A phase 1 study of oral ASP5878, a selective small-molecule inhibitor of fibroblast growth factor receptors 1-4, as a single dose and multiple doses in patients with solid malignancies. Invest New Drugs.
- Yang, C., Lu, W., Lin, T., You, P., Ye, M., Huang, Y., Jiang, X., Wang, C., Wang, F., Lee, M.H., Yeung, S.C., Johnson, R.L., Wei, C., Tsai, R.Y., Frazier, M.L., McKeehan, W.L., Luo, Y., 2013. Activation of Liver FGF21 in hepatocarcinogenesis and during hepatic stress. BMC Gastroenterol 13, 67.
- Ye, Y., Shi, Y., Zhou, Y., Du, C., Wang, C., Zhan, H., Zheng, B., Cao, X., Sun, M.H., Fu, H., 2010. The fibroblast growth factor receptor-4 Arg388 allele is associated with gastric cancer progression. Ann Surg Oncol 17, 3354-3361.